Energy Conversion and Management 269 (2022) 116095

Contents lists available at ScienceDirect

Energy Conversion and Management

journal homepage: www.elsevier.com/locate/enconman

Sustainability analysis of methane-to-hydrogen-to-ammonia conversion by integration of high-temperature plasma and non-thermal plasma processes

Jose Osorio-Tejada [a,g,*], Kevin van't Veer [c], Nguyen Van Duc Long [a,b], Nam N. Tran [b,d], Laurent Fulcheri [e], Bhaskar S. Patil [f], Annemie Bogaerts [c], Volker Hessel [a,b]

[a] School of Engineering, University of Warwick, United Kingdom
[b] School of Chemical Engineering and Advanced Materials, University of Adelaide, Australia
[c] Department of Chemistry, Research Group PLASMANT, University of Antwerp, Universiteitsplein 1, 2610 Antwerp, Belgium
[d] Department of Chemical Engineering, Can Tho University, Vietnam
[e] MINES ParisTech, PSL-Research University, PERSEE, Sophia-Antipolis, France
[f] EU Process Development and Circularity, PSP and HC R&D, The Dow Chemical Company, Hoek, The Netherlands
[g] Territorial Environmental Management Research Group -GAT-, Universidad Tecnológica de Pereira, Pereira, Colombia

ARTICLE INFO

Keywords:
Techno-economic-environmental analysis
High-Temperature plasma
Non-thermal plasma
Methane
Hydrogen
Ammonia

ABSTRACT

The Covid era has made us aware of the need for resilient, self-sufficient, and local production. We are likely willing to pay an extra price for that quality. Ammonia (NH_3) synthesis accounts for 2 % of global energy production and is an important point of attention for the development of green energy technologies. Therefore, we propose a thermally integrated process for H_2 production and NH_3 synthesis using plasma technology, and we evaluate its techno-economic performance and CO_2 footprint by life cycle assessment (LCA). The key is to integrate energy-wise a high-temperature plasma (HTP) process, with a (low-temperature) non-thermal plasma (NTP) process and to envision their joint economic potential. This particularly means raising the temperature of the NTP process, which is typically below 100 °C, taking advantage of the heat released from the HTP process. For that purpose, we proposed the integrated process and conducted chemical kinetics simulations in the NTP section to determine the thermodynamically feasible operating window of this novel combined plasma process. The results suggest that an NH_3 yield of 2.2 mol% can be attained at 302 °C at an energy yield of 1.1 g NH_3/kWh. Cost calculations show that the economic performance is far from commercial, mainly because of the too low energy yield of the NTP process. However, when we base our costs on the best literature value and plausible future scenarios for the NTP energy yield, we reach a cost prediction below 452 $/tonne NH_3, which is competitive with conventional small-scale Haber-Bosch NH_3 synthesis for distributed production. In addition, we demonstrate that biogas can be used as feed, thus allowing the proposed integrated reactor concept to be part of a biogas-to-ammonia circular concept. Moreover, by LCA we demonstrate the environmental benefits of the proposed plant, which could cut by half the carbon emissions when supplied by photovoltaic electricity, and even invert the carbon balance when supplied by wind power due to the avoided emissions of the carbon black credits.

1. Introduction

Ammonia (NH_3) constitutes one of the most important platform chemicals in the synthesis of fertilisers, which further supports global crop production. Besides its relevance in agriculture, NH_3 has recently been proposed as an energy vector, given its greater ease of storage and transport than pure hydrogen (H_2) [1–3]. Yet, at an industrial level, NH_3 manufacture is associated with high energy consumption and carbon emissions due to its dependence on fossil resources to produce the H_2 feedstock, mainly via the steam methane reforming (SMR) process, required to synthesize the NH_3 through the conventional Haber-Bosch (HB) process. Moreover, the HB process has almost reached its theoretical efficiency, being economically unfeasible to continue investigating how to improve this process [4,5]. In view of the projected population increase by 2050 and the ever-increasing environmental concerns about industrial emissions, sustainable techniques for the synthesis of NH_3 need to be adopted, with the focus being placed on employing renewable raw materials and improving energy efficiency [6].

* Corresponding author.
E-mail address: jose.osorio-tejada@warwick.ac.uk (J. Osorio-Tejada).

https://doi.org/10.1016/j.enconman.2022.116095
Received 16 May 2022; Received in revised form 2 August 2022; Accepted 3 August 2022

Nomenclature

Acronyms

ACC	Annualised capital cost
ACCR	Annual capital charge ratio
CB	Carbon black
CED	Cumulative energy demand
CExD	Cumulative exergy demand
CEPCI	Chemical engineering plant cost indexes
CH_4	Methane
CO	Carbon monoxide
CO_2	Carbon dioxide
DBD	Dielectric barrier discharge
HB	Haber-Bosch
HTP	High-temperature plasma
IPCC	Intergovernmental panel on climate change
LHV	Lower heating value
LCA	Life cycle assessment
MMBTU	Metric million British thermal units
NG	Natural gas
NH3	Ammonia
NOx	Nitrogen oxides
NTP	Non-thermal plasma
PNOCRA	Plasma nitrogen oxidation and catalytic reduction to ammonia
PSA	Pressure swing adsorption
SEI	specific energy input
SMR	Steam methane reforming
TEA	Techno-economic analysis
UCOP	Unitary cost of production

The Covid era [7] and global shortages [8] have amplified a recent change in the economic model [fractal] to resilient, self-sufficient, and local production. This is in the background of the United Nation's "Building Back Better concept" [7]; quoting: "Using new technologies, the local and regional levels have become key spaces for experimentation and innovation, …". This economic switch has been termed 'fractal economy' [9]. While this as such generates higher costs, since smaller distributed plants cannot reach the economics of their global-market-supplying giants, it offers opportunities in benefitting from additional revenue through local market opportunities, such as the creation of additional jobs, co-valorisation only possible in close proximity (e.g., using local resources to upgrade the NH_3 product), carbon credits to account for cleaner production, better use of resources (the major part of current fertilizers are washed out), and less soil degradation.

An alternative way for the distributed production of H_2 and NH_3 is plasma technology. Plasma-based processing allows making chemical activation, both at relatively low and high temperatures, depending on the application. As there is access to renewable energies at many locations, including rural sites, and modularization can help in capacity flexibility and campaign manufacturing, plasma processing can be installed in principle anywhere; thus, supporting the alternative economic model of distributed fertilizer production [10]. Plasma processing has recently made major steps toward industrial capacity; at least what concerns high-temperature plasmas, so-called thermal plasmas.

Thermal plasma methane (CH_4) pyrolysis is one of the recently industrialised innovative processes in which CH_4 is split into H_2 and solid carbon, without airborne carbon emissions [11–13]. Another route to synthesize H_2 by means of hydrocarbon reforming in high-temperature plasma reactors with high energy efficiency is the glycerol steam reforming [14], which has been realized in a thermal direct current arc discharge reactor at various operating conditions [15]. For a feed ratio ($H_2O/C_3H_8O_3$) of 1.1 the highest H_2 yield of 78.5 % and carbon conversion of 91.4 % were attained. At the given experimental conditions, the energy efficiency of the specific thermal process was estimated at 0.527 kWh/kg H_2. Besides glycerol, methanol was also explored as a feedstock for H_2 production in a heat-insulated thermal plasma reactor [16]. In the absence of catalysts, the plasma process exhibited a maximum methanol conversion of 50 % for a specific energy input (SEI) of 80 kJ/mol. In addition, when Fe-Cu/γ-Al_2O_3 catalyst was incorporated, an improvement in the methanol conversion towards 88 % was observed, with an energy efficiency of 9.5 kWh/kg H_2 (0.85 kWh/Nm^3). Moreover, CH_4 steam reforming in a thermal plasma torch was also examined at an operating temperature of 1100 °C. At an H_2O/CH_4 feed ratio of 1.23, the H_2 yield reached up to 50.4 % with an energy density of 0.017 kJ/L [17].

Low-temperature plasma processes lack behind those industrial successes. Yet, strong academic interest and developments show promising potential [18]. The plasma-catalytic synthesis of NH_3 in non-thermal plasma (NTP) reactors has been mostly explored at relatively low operating conditions, i.e. ambient temperature and pressure [19–25]. Among different kinds of NTP reactors, such as glow discharge, microwave plasma, radio frequency discharges, plasma-liquid systems, arc discharges, and dielectric barrier discharge (DBD) reactors, the latter has been the most increasingly studied for NH_3 production, due to its flexibility and its ease of allowing the integration of catalysts [25]. Indeed, the highest energy yield obtained so far (35.7 g NH_3/kWh) was in this kind of DBD reactor at 300 °C [26]. However, a few studies also evaluated the plasma-chemical reaction at slightly higher temperatures, above 100 °C. More precisely, Rouwenhorst et al. [27] have evaluated the activation energies of plasma-catalytic NH_3 synthesis over an alumina-supported ruthenium catalyst at temperatures ranging from 200 °C to 330 °C. For the given temperature range, a synergetic effect was detected between the employed catalyst and plasma, accompanied by lower activation energies – from 20 to 40 kJ/mol – as compared to the thermal catalytic NH_3 synthesis. Furthermore, Shah et al. tested the NH_3 synthesis over a set of metal-based catalysts at 400 °C [28], and molten Ga as catalyst demonstrated the highest NH_3 yield of 10 % and an energy yield of 0.22 g-NH_3/kWh.

Hardly any of the plasma-based NH_3 synthesis works have considered the H_2 feed as the true cost and environmental driver of any sustainable NH_3 synthesis. A novel concept was, however, recently proposed for plasma-based NH_3 production, called PNOCRA (i.e., Plasma Nitrogen Oxidation and Catalytic Reduction to Ammonia) [29]. It is a combination of plasma-based NO_x formation from air, with Lean NO_x Trap technology, adopted from diesel engine exhaust gas after-treatment technology, on which the adsorbed NO_x is periodically reduced with green H_2 to NH_3. Process modelling showed that PNOCRA achieves an energy requirement of 4.6 MJ/mol NH_3 (i.e., 270 GJ/t NH_3), which is an over 4-fold energy reduction compared to the state-of-the-art plasma-catalytic NH_3 synthesis directly from N_2 and H_2 with reasonable yield (>1%). Furthermore, there is still room for improvement, by optimizing the plasma-based NO_x process [30]. Indeed, recent experiments with a pulsed plasma jet yielded record-low energy costs for NO_x production of 0.42 MJ/mol NO_x [31], which reduced the energy cost of the PNOCRA process down to only 2.1 MJ/mol NH_3 [32]. We believe this is the lowest energy cost for decentralized small-scale green ammonia production reported so far.

In the present paper, we propose a novel concept, namely the thermal integration of thermal and non-thermal plasmas, by allowing the hot thermal plasma effluent to enter the 'non-thermal plasma' without (complete) cooling down; in this way, effectively turning the second reactor section to 'warm plasma'. In this approach, one needs to propose both H_2 manufacturing technology and NTP process that mutually suit each other and upgrade the joined performance, to allow finally a

foresight to commercial use. Considering this knowledge gap, we propose here a novel process design for the NH_3 synthesis by means of integrating high-temperature plasma (HTP) and NTP technologies via a hot HTP effluent stream. In this way, methane or even biogas can be converted to H_2 as feedstock for NH_3 synthesis.

The main opportunity to demonstrate in this paper is that heat integration is a viable (economic) process concept. That inevitably necessitates performing the NTP step at higher temperatures than have been investigated so far. Accordingly, this feasibility has been checked by plasma chemical kinetics simulations considering various catalysts, and optimum operating conditions of the NTP-based NH_3 production are determined. In turn, this has motivated a study on evaluating the energy performance of the HTP process under different operating conditions and biogas compositions. This adds to the insight already gained with pure methane, originating from steam processing using NG as a non-renewable resource, yet resulting in a CO_2-footprint favourable process coined as "turquoise hydrogen".

Our approach yields a new paradigm, i.e., that NTP chemical processes should not always be operated at as low temperature as possible to save energy. This common statement is made based on analysing the plasma-chemical process alone without consideration of upstream processes. Such statement can be biased and ignores alternative solutions being better in the overall material and energy use. Given that upstream processes can be – favourably – of high temperature, the question arises how to make the best use of that large pool of energy and to create secondary opportunities. Thus, we propose here to operate the NTP process at higher temperatures; yet still with the goal to optimise the energy efficiency. Selected process design scenarios are also appraised with respect to critical process parameters, aiming to identify potential hotspots in the proposed process design and support future decision-making.

2. Methods

The production of H_2 by means of HTP technology was modelled in Aspen Plus software [33]. Plasma chemical kinetics simulations for the synthesis of NH_3 in a DBD reactor (NTP) have been conducted for a set of catalysts, aiming to identify the best operating window for this novel process design, with respect to product yield, operating temperature, and energy input. These simulations were built in the Zero-Dimensional Plasma Kinetics solver ZDPlasKin [34,35] by considering the high-temperature H_2 stream generated from the HTP process. We detailed an integrated HTP-NTP process for NH_3 production at warm temperatures and atmospheric pressure, using electricity as the only external energy source. We also conducted a techno-economic analysis (TEA) and life cycle assessment (LCA) of the integrated HTP-NTP system for an NH_3 production rate of 13 tonnes/h (~106,000 tonnes/year), which would supply the demand of specific regions in farming dispersed areas [36]. This capacity for regional supply can be considered an intermediate capacity between local- and world-scale production for bulk-scale chemicals [10]. This NH_3 production volume is in the range of the H_2 yearly production capacity of the current and planned HTP industrial-scale plants [37]. Moreover, we included in these analyses the costs and emissions reduction due to the sales of solid carbon (carbon black – CB), a co-product of the HTP process. We additionally conducted scenarios analyses based on energy efficiencies of plasma-assisted NH_3 synthesis from literature, and we also used optimistic foresights to analyse the economic and environmental performance of these novel technologies in the future. A brief description of the HTP modelling, NTP chemical kinetics simulations, and the integrated HTP-NTP process design is provided below.

2.1. HTP: high-temperature plasma-assisted H_2 production

Methane can decompose to C and H_2 at high temperatures (1500–2000 K). The required temperature level, however, involves the use of an appropriate, sustainable energy supply; meaning heating the gas at 2000 °C without CO_2 emission. Conventional heating has not shown to accomplish that. For example, graphite Joule heating did not function technologically and was inefficient at large scales due to carbon fouling issues. Thermal plasma remains the only method having proven sustainable heating, with negligible CO_2 emissions [11]. The production of H_2 by means of HTP technology was modelled in Aspen Plus software, based on the process model and operating conditions described by Sarafraz et al. [36]. As shown in Fig. 1 (upper part), the biogas stream, consisting of CH_4 and CO_2, is fed into the thermal plasma reactor, which comprises two reaction zones to obtain a high chemical yield of the HTP reactor. The main purpose of zone 1 is to convert electrical energy to thermal energy, while the purpose of zone 2 is the production of H_2 and CB. Firstly, the produced biogas enters zone 2 to produce H_2, CB, and carbon monoxide (CO). Then, the outlet stream from the HTP reactor is used to preheat the biogas feed to 600 °C before being fed into a separator to separate CB, H_2, and CO. A fraction of H_2 or both H_2 and CO is recycled to zone 1 to produce H radicals at 3000 °C, via the reaction $H_2 => 2H$ using electricity, before entering zone 2 for H_2 and CB production at 1500 °C via the reaction $CH_4 => C + 2H_2$. Note that, for modelling the HTP-assisted hydrogen production, the universal quasichemical -UNIQUAC - properties package was employed. As the reactions happen very fast at high temperatures and the reaction set is very complicated, RGibbs based on the concept of equilibrium reaction estimation to minimize Gibbs free energy was used to simulate the thermal plasma reactor.

2.2. NTP: non-thermal plasma-assisted NH_3 synthesis

2.2.1. Non-thermal plasma chemical kinetics simulations

The NTP-based NH_3 synthesis was assumed to take place in a DBD plasma reactor, which for gas conversion typically operates in a filamentary regime [38]. To get a concise indication of the performance, simulations were performed over a large range of catalysts (Fe, Ru, Co, Ni, Pt, Pd, Cu, and Ag) and temperature (from approximately 25 °C to 725 °C), i.e., ranges that are larger than readily available from specific (experimental) literature [21,24,27,39]. In addition, based on literature a fixed feed gas ratio of N_2:H_2 = 2:1 was assumed, i.e., favouring N_2, as it is known that the optimal feed gas ratio for plasma-catalytic NH_3 synthesis deviates from the expected stoichiometric optimum (N_2:H_2 = 1:3) [26]. The model was built in the ZDPlasKin solver [34,35], and previously reported in detail [40,41]. Briefly, a continuity equation was solved for each type of plasma species in the plasma reactor, which is represented here as a batch reactor, such that by solving the continuity equation, the time dependency directly represents the residence time [42]. In turn, the residence time together with the reactor volume can directly be related to a wide range of SEI values in the plasma, given by the plasma power times the residence time and divided by the reactor volume. 70 different species (including various vibrational levels of H_2 and N_2), approximately 4,000 different chemical reactions in the plasma phase [41], and 19 reversible surface reactions [43] at the catalyst surface (including dissociative adsorption, radical adsorptions, and Langmuir-Hinshelwood and Eley-Rideal type reactions) were included in the model.

The SEI is determined by the ratio of plasma power over the gas flow rate. The average plasma power was taken as 68 W [41]. An accurate description of the filamentary behaviour in the DBD reactor volume was achieved by considering the average pulse shape of the instantaneous power characteristics [34,38,41]. A number of filamentary micro-discharges were considered as a function of time, to capture the average behaviour of the plasma reactor [40].

The maximum instantaneous power was 294 W, and the minimum instantaneous power was 33 W. This is translated to a power density of 3.4×10^6 and 12 W/cm^3, respectively. The reactor volume was taken as 20 cm^3 and a micro-discharge volume of 8.8×10^{-5} mm^3 was assumed [41]. Finally, the lifetime of the filamentary micro-discharges was

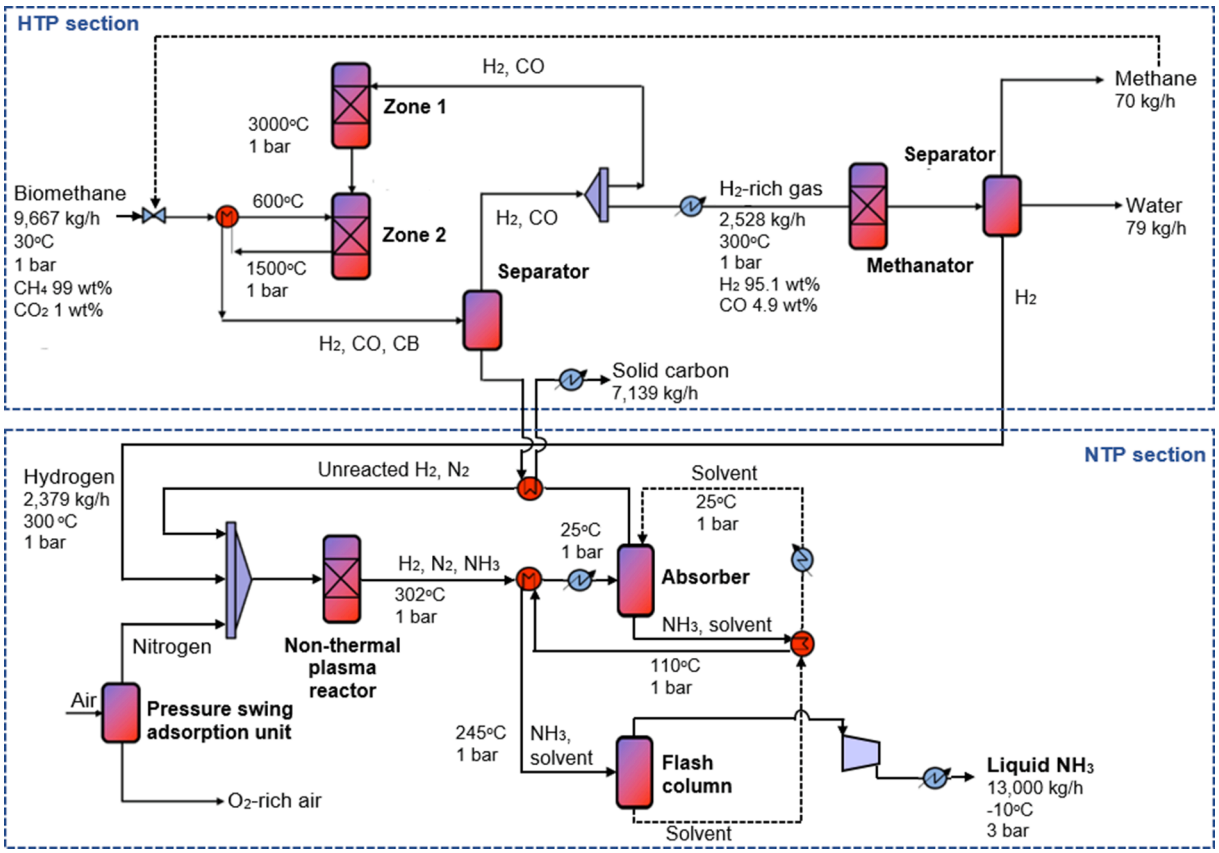

Fig. 1. Process flowsheet of integrated plasma-assisted biomethane-to-H2-to-NH3 synthesis, based on HTP (upper part) and NTP (lower part).

assumed as 200 ns. The power density determines the plasma characteristics, as the power is transferred to the electrons through Joule heating by the electric field. These plasma characteristics are typically observed in experiments, as a function of the plasma power, reactor dimensions, packing, and catalyst and support material [24,44].

2.2.2. *Non-thermal plasma-assisted NH_3 synthesis process model*

Based on the plasma chemical kinetics simulations discussed above, the NTP-based NH_3 synthesis was considered to take place in a DBD reactor at the operating conditions at which the maximum NH_3 yield was attained. According to these simulations, the highest NH_3 energy yield seems to be achieved at 302 °C and 1 bar for an N_2/H_2 feed molar ratio of 2:1, employing a Fe surface catalyst. The conceptual design of the NTP plasma process is illustrated in Fig. 1 (lower part). NH_3 separation/purification is performed at 25 °C and 1 bar using an ionic-liquid-based solvent as proposed by Anastasopoulou et al. [45,46], who considered a 1.0 mol% NH_3 concentration. In their method, external heating is needed to recover the ionic liquid. However, we save part of this energy expenditure by using the heat of the outlet gas of the NTP reactor to preheat the NH_3/ionic liquid mixture before being separated in the flash column, and thereafter, it is cooled down to obtain the pure liquid NH_3.

2.3. *Techno-economic analysis*

The economic analysis involves the estimation of the production cost based on process equipment and material/energy consumption in the H_2 and N_2 production and NH_3 synthesis processes. In order to provide meaningful insights into the economic performance and profitability of the integrated HTP-NTP process, we present a comparative assessment of our novel process with the stand-alone (electrolyser-based H_2 production) for NTP plasma-catalytic NH_3 synthesis process, as well as compared with a scaled-down conventional SMR-HB process [45,46].

The cost of the reactors and auxiliary equipment for the HTP section were based on data from Labanca [47], who reported an investment of 80 million US$ for a plant with a capacity of 6,571 t H_2/year in 2020. The cost of the NTP reaction section was based on Dobslaw et al. [48], who reported, for a 40 kW system, investments of 56,000 US$ for the NTP stacks and 60,000 US$ for the NTP power supply in 2017. The cost of the proton exchange membrane electrolyser for the stand-alone NTP plant was based on NREL 2019 [49], who reported an investment of 460 US$/kW for a 119,000 kW plant in 2016, also considering a 15 % replacement cost every 7 years due to the stack degradation. The cost of the pressure swing adsorption (PSA) unit for nitrogen generation was based on a reported cost of 100,000 US$ for a 3-tonne N_2/day unit [50]. These costs from literature were updated to US$2020 using the chemical engineering plant cost indexes (CEPCI) [51] and the scaling factor exponent of 0.8 for electrolysers [52,53] and 0.6 for the rest of the equipment [54].

The power consumption of the HTP reactor system ($Q_{zone\ 1}$ = 3.31 MW, $Q_{zone\ 2}$ = 51.49 MW) was 24.7 kWh/kg H_2 (i.e., 40.5 g H_2/kWh energy yield) based on the 54.8 MW to produce the usable 2,379 kg H_2/h, plus 2.9 kWh/kg H_2 for the auxiliary equipment required to run the system and the downstream treatments, such as H_2 purification and CB handling. For the NH_3 synthesis, two scenarios were evaluated, i.e., (i) considering energy yields of 1.1 g NH_3/kWh, as dictated by the plasma chemical kinetic simulations; (ii) 35.7 g NH_3/kWh, as the maximum energy yield reported for plasma-catalytic NH_3 synthesis in literature [26]; and (iii) the theoretical maximum energy yield of 900 g NH_3/kWh [55,56]. A concentration of 1.0 mol% NH_3 was assumed in all the analysed scenarios, which is an average concentration obtained in most of the studies on plasma-catalytic NH_3 production [25,39], and it would be an acceptable rate to have low energy costs for the separation and recycling loops of unreacted H_2/N_2 [25,57].

The cost of the electricity was $0.05/kWh for onsite generation based on Fasihi et al. [58], who showed that photovoltaic electricity in Australia can cost between 0.02 and 0.03 €/kWh and wind electricity between 0.03 and 0.05 €/kWh in 2020, decreasing by half of the cost in 2050. The other utility costs, such as process water, heat, and steam, were estimated according to the Ulrich 2006 method [59], based on a NG price of 4 $/MMBTU. For sensitivity analysis, we also estimated the variation of NH_3 production costs due to the volatility of NG, electricity, and co-products prices.

In terms of the catalyst used in the plasma-catalytic NH_3 synthesis, we assumed a synthesis rate of 1,037 μmol/g catalyst/h and a Fe surface catalyst cost of $15.5/kg, amortized over a period of 5 years, which is equivalent to 0.0014 kg catalyst/kg NH_3. The cost of the absorber, column, compressor, and heat exchangers for the NH_3 separation was based on Anastasopoulou et al. [46], requiring about 28 GJ/t NH_3 of cooling energy, equivalent to 1.27 kWh/kg NH_3 using an electric chiller, which consumes 0.58 kW per tonne of refrigeration [60,61], plus 0.082 kWh/kg NH_3 for compression. Regarding labour costs, a total of 8 operators were calculated based on the reported requirement of 2 operators for a stand-alone NTP plant with capacity of 340 tonne/year [46] and using a 0.25 scaling factor exponent [62].

Given that the CB is a valuable co-product of the HTP section with increasing demand, mainly for tires and industrial rubbers, with current global prices over 1,000 $/t [63], these CB sales were included as credits in the economic analysis, to reduce the costs of the main NH_3 production.

The unitary cost of production (UCOP) was estimated based on the annualised capital cost (ACC) method [64], as shown in the following equations:

$$\mathrm{UCOP} = \frac{Opex + ACC}{annual\ \ plant\ \ capacity} \tag{1}$$

$$ACC = ACCR \times total\ \ fixed\ \ capital\ \ cost \tag{2}$$

$$ACCR = \frac{[i(1+i)^n]}{[(1+i)^n - 1]} \tag{3}$$

Opex corresponds to the annual operating costs, which consist of variable and fixed operating costs. These fixed operating costs, as well as the total fixed capital cost, were estimated through a factorial approach based on percentages of the non-installed equipment costs [62]. The ACC (or Capex) are obtained using the annual capital charge ratio (ACCR), calculated as a function of a 10 % interest rate (i) and a 15-year lifespan of the plants (n). A downtime period of 600 h/year (i.e., equivalent to 340 productive days per year) was considered for all the analysed plants.

2.4. Environmental assessment

Since one of the main issues of conventional NH_3 production is the use of fossil fuels and its consequent emanation of almost 2 % of the global anthropogenic CO_2 emissions [65], we assessed the life-cycle emissions of the NH_3 production for the different analysed pathways.

For this purpose, we applied the LCA methodology [66] and focused on the global warming impact category for the analysis of the CO_2 equivalent emissions per tonne of NH_3 as functional unit. The system was based on the cradle-to-gate scope, using a cut-off model, and considering mass allocation. Given that different pathways generate co-products, such as CB, or by-products, such as steam, these credits were accounted for under the approach of "avoided burden" or system expansion [67].

The life cycle inventories were developed for the specific case of Australian energy sources based on datasets from Ecoinvent 3.8 [68]. The impacts assessment was performed using SimaPro 9.2 [69] and the method IPCC 2013 [70], considering the 100-year time horizon and excluding long-term emissions.

The conventional SMR-HB route and the alternative pathways were initially analysed using fossil energy sources and electricity from the Australian grid. Subsequently, the alternative pathways were analysed by using solar and wind electricity, as well as biogas to feed the HTP section. The summarised operating parameters for the TEA and LCA of the different NH_3 production pathways are presented in Table 1.

Additionally, we calculated the total energy consumption per tonne of NH_3 as an indicator of the efficiency of the plant. Yet, each pathway uses different types of energy, with different physical and thermodynamic properties. Hence, it is not appropriate to sum up or compare the quantity of MJ of heat or cooling energy with the equivalent MJ of electricity, generated from different fossil or renewable resources in power plants with diverse efficiencies. For this reason, it was necessary to obtain these indicators using the life cycle impacts assessment methods Cumulative Energy Demand (CED) [71] for the lower heating values (LHV) of the energy sources, as well as the Cumulative Exergy Demand (CExD) [72], which consider the primary energy expenses for all the life cycle phases, including the expenses for the manufacturing of equipment required for the transformation and use of the energy inputs.

Table 1
Operating parameters for the stand-alone NTP, HTP-NTP, and SMR-HB plants for ammonia production.

Parameter	Stand-alone NTP	HTP-NTP [a]	SMR-HB
Hydrogen generation section			
Electricity (kWh)/ kg H_2	55.50	27.60 [b]	0.59
NG (MMBTU)/ kg H_2		0.21	0.09
Process water (kg)/kg H_2	14.31 [c]		37.41
Cooling energy (MJ)/kg H_2			52.63
Heat (MJ)/kg H_2			86.36
Steam (kg)/kg H_2			−28.05
Hydrogen sulphide (g)/kg H_2			−0.04
Carbon dioxide (g)/kg H_2			−0.51[d]
Carbon black (kg)/kg H_2		−3.00	
Nitrogen generation section			
Electricity (kWh)/kg N_2	0.11	0.11	[e]
Ammonia synthesis and separation sections			
Electricity (kWh)/kg NH_3	1,250 [f]	1,250 [f]; 917 [g]; 28 [h]	0.40
Cooling energy (MJ)/kg NH_3	28 [i]	28 [i]	3.89
Heat (MJ)/kg NH_3	3.90		0.05
Process water (kg)/kg NH_3			0.94
Steam (kg)/kg NH_3			−0.94
Hydrogen (g)/kg NH_3			−7.77

Notes: Ratio $NH_3/H_2 = 5.11$ (HB process); 5.52 (NTP process). Ratio $NH_3/N_2 = 1.17$. These ratios are used to convert values per H_2 and N_2 in values per NH_3. Catalysts usage rates are detailed in the operating costs tables in the Supplementary Material file.
(a) Parameters for the integrated HTP-NTP plant detailed in Fig. 1, which considers post-treatment for CO removal using methanation. The parameters for a variation of this plant using pre-treatment for the CO_2 removal in methane input, instead of post-treatment of CO, are detailed in section 3.3.4. (b) An electricity consumption of 1.82 kWh/kg H_2 must be added in the scenario of using a methane pre-separation technology (as described later in section 3.3.4), i.e., using a membrane-based separator before the HTP reactors. (c) Deionised water. (d) It corresponds to the CO_2 removed from the NG input, it is not CO_2 removed from air combustion emissions by carbon capture, utilisation, and storage (CCUS) systems. (e) Included in the consumption of electricity (kWh)/kg H_2. (f) Non-integrated plant: 0.8 g NH_3/kWh. (g) Integrated HTP-NTP: 1.09 g NH_3/kWh. (h) Integrated HTP-NTP; 35.7 g NH_3/kWh. (i) Cooling energy used in the NH_3 separation was produced by electric equipment (chiller/heat exchanger), with consumption of 1,29 kWh/kg NH_3, plus 0.082 kWh/kg NH_3 for the recycling loop and the final compression/condensation.

3. Results and discussion

3.1. Demonstration of performing the HTP process with biogas and optimization of this process

The distributed production close to the consumer site improves resilience, self-sustainment, and local benefits; finally aiming at a circular system. The whole angle of view is taken from the needs of farmers in a country like Australia, with very large transport distances and needs for a food market under the current geopolitical environment.

With large resources available concerning animal and crop waste, biogas has become attractive as a source of renewable CH_4. In this sense, we investigated the feasibility of using biogas, i.e., CO_2-diluted CH_4, as renewable feedstock instead of using pure CH_4 for H_2 production. That would allow to add the resources from the food and Agtech industries themselves, rather than taking fossil resources (steam reforming) or hybrid solutions (electrolysers). The very right solution then would be the thermal plasma process. Yet, this asks for optimization towards the new feed biogas.

In this context, we investigate the feed of biogas into the thermal plasma reactor, which commonly operates with two reaction zones (see Fig. 1).

3.1.1. Proof of the approach - effect of HTP feed composition

If biogas really is to be used for the HTP process, pure or as a mixture with NG, the impact of the HTP feed composition (CO_2/CH_4) must be analysed in terms of product amount and total duty. Biogas is mainly composed of CH_4 (50 % – 70 %) and CO_2 (30 % – 50 %) [73]. Thus, four cases with different conditions, depending on the separation step prior to the HTP reaction, were simulated.

- Case 1: Complete separation: 100 % CH_4 and 0 % CO_2.
- Case 2. Nearly complete separation: 99 % CH_4 and 1 % CO_2.
- Case 3. Limited separation: 90 % CH_4 and 10 % CO_2.
- Case 4. No separation: 70 % CH_4 and 30 % CO_2.

Fig. 2 shows the effect of the CO_2 concentration on the amount and the ratio of products when CO is not recycled. The H_2 yield decreases in a linear fashion. Yet, this demonstrates that our main assumption was right, i.e., that notable H_2 amounts can be produced by thermal plasma with biogas feed. The question then arises whether the lowering is just due to H_2 dilution or another effect, and this is answered below. The CO_2 is not inert under these conditions and rather reacts to decompose to CO and O_2. It should be noted that no O_2 is left in the reaction mixture, meaning it is completely consumed by CB oxidation. The CO content increases for cases 1–4, in accordance with their higher CO_2 feed load. The CB amount drops linearly, as it is oxidised by O_2 to give CO_2. The loss in O_2 and CB yield is partly compensated by a lower energy demand, as expressed by the total duty being reduced from 55.23 MW to 42.31 MW from case 1 to case 4, respectively, thanks to the smaller amount of CH_4 reactant.

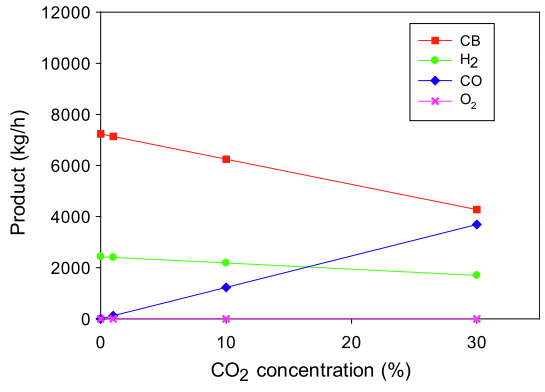

Fig. 2. Effect of the CO2 concentration (cases 1–4 mentioned in the text) in the biogas feed on the production rates of the various products. Note: Outputs of the HTP process considered in the scheme in Fig. 1 correspond to case 2 (CO2 1 wt% on the x-axis), with production rates of 2,404 kg H2/h, 124 kg CO/h, and 7,139 kg CB/h.

We investigated the question if there might be a loss of H_2 by oxidation with CO_2 or if the lower H_2 yield of cases 2–4 is just a matter of dilution with CO_2. For this purpose, we considered another case without CO_2, while the CH_4 specific flow rate is the same as in case 4 (70 % CH_4 and 30 % CO_2), meaning to normalise the dilution effect by increasing the total flow rate correspondingly. It turns out that both cases produce the same amount of H_2 (1,700.6 kg/h) at 2500 °C. This means that there is no H_2 oxidation upon the presence of CO_2 and the lower H_2 flow rate for cases 1 to 4 is only caused by the CO_2 dilution. It has to be admitted that the dilution effect demands for an increase in the reactor volume, which raises capital investments. Yet, the negative news is that some of the high-value product CB is lost by oxidation with O_2 to give CO_2.

When both H_2 and CO are recycled, the duty in zone 1 increases, leading to a slight increase in the total duty as compared to when CO is not recycled. Furthermore, the product quantities are kept constant as compared to the case where only H_2 is recycled, and the plasma can run very well with a mixture of CO/H_2.

To sum up, two main outcomes are shown, which are (i) the possibility to produce H_2 from biogas and (ii) the concurrently removing all the CO_2 content for the benefit of zero-emission of CO_2 as a greenhouse gas to the environment.

3.1.2. Effect of temperature of zone 2

Here, we investigate the effect of the temperature because this is responsible for the high energy costs. Any improvement here will help the economy of the HTP-NTP process. Since the temperature of zone 1 does not affect the total efficiency [36], we varied only the temperature of zone 2. This analysis was applied to the case 4 composition to check the sensitivity of the process when the feed has a high CO_2 content. Fig. 3 shows that when the temperature of zone 2 increases from 700 °C to 2500 °C, the conversion of CH_4 and CO_2 increase from 79 % to 100 % and from 91 % to 100 %, respectively, and the CB and H_2 yields increase from 75 % to 85 % and from 75 % to 100 %, respectively. It can be also seen that for these conversions, most conversion takes place at the beginning when the temperature rises from 700 °C to 1200 °C. Subsequently, the conversions remain stable when the temperature continues to rise. Because the duty rises linearly with temperature, a higher temperature would not be beneficial. Therefore, temperatures between 1100 °C and 1500 °C can be employed in the design of the HTP reactor. Note that the H_2O amount reduces from 744.8 kg/h to 0.1 kg/h when the temperature of zone 2 rises from 700 °C to 2500 °C. The presence of CO_2 does not harm the H_2 production, although it decreases a bit the activated carbon outcome.

With these simulations, we also demonstrate that C and H_2 can be produced even from 700 °C. For this reason, we only preheat the feed until 600 °C to avoid that the reaction can occur in the heat exchanger and pipes before the zone 2 reactor (see Fig. 1).

3.2. Demonstration of performing the NTP process at higher temperatures

3.2.1. Results of the NTP chemical kinetics simulations

To assess the potential performance of the NTP, various metal catalyst surfaces were simulated in a DBD plasma environment. The calculations were performed over a residence time of up to 4 s, corresponding to a SEI up to 27.2 kJ/L, with a feed gas ratio of N_2:H_2 = 2:1, and over a temperature range of 25 °C to 725 °C. The final NH_3 concentrations and energy costs are presented in Fig. 4.

NH_3 concentrations between approximately 0.8 mol% and 2.2 mol% are obtained for temperatures below 500 °C (Fig. 4a), with corresponding energy costs between 50 and 100 MJ/mol NH_3 (i.e., ca. 3,000–6,000 GJ/t NH_3) (Fig. 4b). However, starting around 350 °C, the NH_3 concentration drops, and the energy cost increases rapidly. This

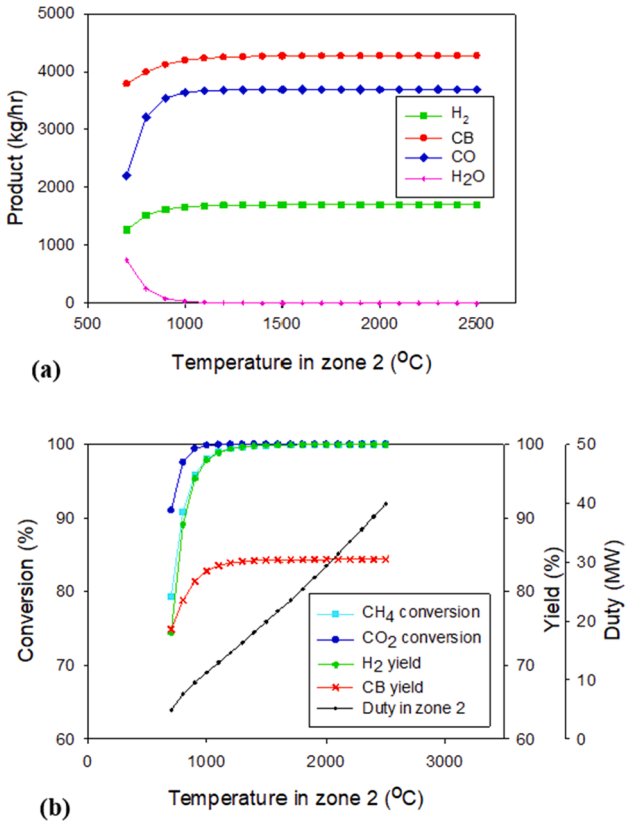

Fig. 3. Effect of the temperature of the thermal plasma – zone 2 on (a) the production rates of the various products and (b) the CH_4 and CO_2 conversion (left y-axis) and the H_2 and CO yield and the duty in zone 2 (right y-axes). Note: the feed composition is CH_4 70 wt% and CO_2 30 wt% (case 4).

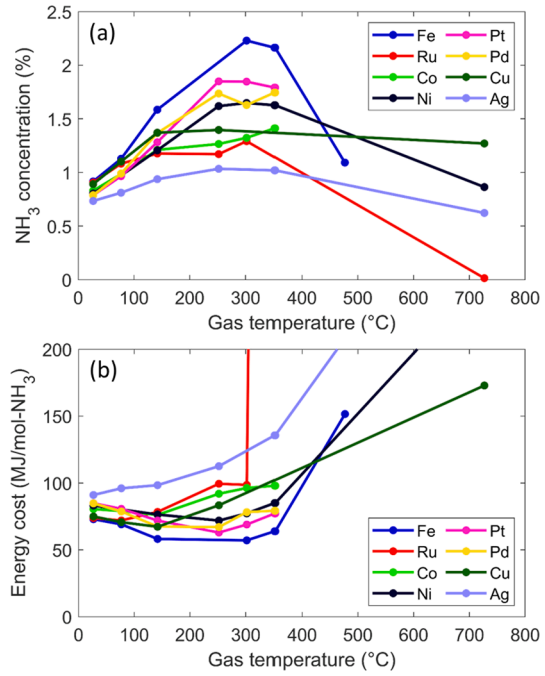

Fig. 4. NH_3 concentration as a function of the gas temperature in the NTP (a) and the corresponding energy cost (b). For some catalyst materials, the calculations could only be performed up to 350 °C, because of negligible conversion.

increase in the energy cost can be understood by the gas density, which is lower at higher temperatures when the pressure remains atmospheric, thus the number of moles NH_3 created in a fixed reactor volume and within a fixed residence time (i.e., assuming a single volumetric flow rate, irrespective of the temperature) is lower, even for the same relative NH_3 concentration. Ru shows a very rapid increase in energy cost from 300 °C to 725 °C (three orders of magnitude; out of range in Fig. 4b), as the concentration drops to 0 mol% at 725 °C.

After 4 s of residence time, the highest NH_3 concentration of 2.2 mol % is obtained at 302 °C on a Fe surface at an energy cost of 56.5 MJ/mol NH_3 (i.e., 3,300 GJ/t NH_3). The effects of residence time for the various metal surfaces are presented in Fig. 5 and Fig. 6 for the evolution of the NH_3 concentration and the corresponding energy cost and NH_3 synthesis rate, respectively, at the temperature at which the best results were obtained for most of the catalysts in Fig. 4 (302 °C).

From Fig. 5, it is clear that the Fe surface is closest to reaching a steady state, and that the NH_3 concentration on the remaining surfaces is still increasing significantly with residence time. We note that for those catalyst surfaces, the steady state is expected to occur at a very high residence time, corresponding to very low flow rates and thus high specific energy inputs into the system, leading to higher energy costs, thus the benefits of a possible higher NH_3 concentration on the other metals will be offset by a higher energy cost.

Fig. 6 shows an initial high energy cost at very short residence time. Here the residence time is too short, i.e., corresponding to a very high flow rate, which does not allow the gas to react sufficiently before leaving the reactor. As the residence time increases, the energy cost decreases, and the synthesis rate rises. With longer residence time, the rise in synthesis rate becomes more modest or even decreases (for Fe, which reaches its steady state earlier in time; cf.). Consequently, the energy cost will start to rise. This is because once a steady state is reached, a longer residence time does not allow for further conversion, hence the extra SEI into the system would only be wasted and not be used for further NH_3 production.

Thus, our model shows that under our specific conditions (i.e., a feed gas ratio of N_2:H_2 = 2:1 and the specific plasma conditions, cf. section 2.2.1), Fe outperforms Ru, while Ru might be expected to outperform Fe instead [74]. Indeed, Mehta et al. [74] have shown that Ru is more active than Fe in both thermal catalysis and plasma-enhanced catalysis. However, they did not consider all possible plasma-surface interactions. Recently, the effect of radical adsorptions and elementary Eley-Rideal processes was studied. It was found that those processes significantly reduce the difference in activity between the various metal catalysts [43]. Those observations were later supported by experiments. In the latter study, different feed gas ratios were considered, i.e., N_2:H_2 = 1:3, 1:1, and 3:1. For the latter feed gas ratio, Fe was found to outperform Ru [75].

In conclusion, our plasma chemical kinetics simulations predict that the highest NH_3 concentration of 2.2 mol% is obtained at 302 °C on a Fe

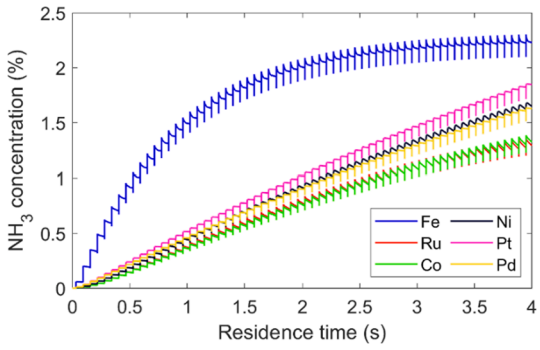

Fig. 5. NH_3 concentration as a function of residence time for various catalyst surfaces at 302 °C.

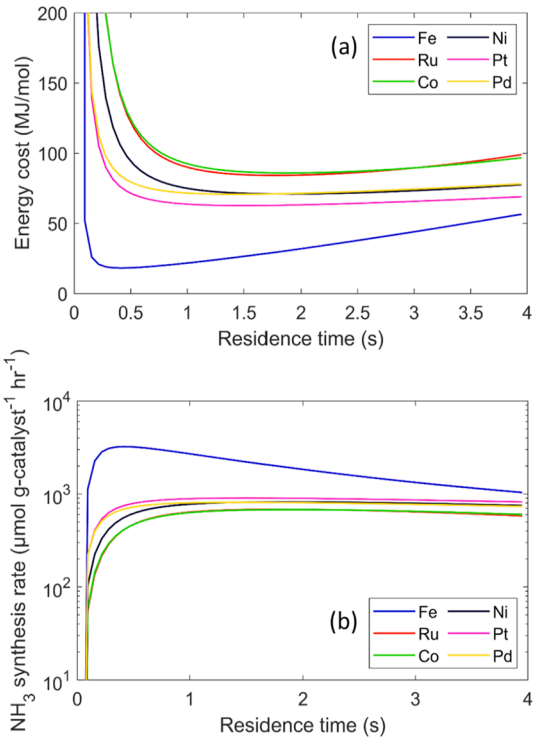

Fig. 6. Energy cost of NH_3 formation (a) and the corresponding synthesis rate (b) as a function of residence time for various catalyst surfaces at 302 °C.

surface at an energy cost of 3,300 GJ/t NH_3. This corresponds to an energy yield of 1.1 g NH_3/kWh. These numbers are used in the economic assessment of the stand-alone NTP and the integrated HTP-NTP process.

3.2.2. *Performance of NTP-assisted ammonia synthesis*

Different plasma reactors are able to convert the input power to different field intensities, with different spatial and temporal distribution, and different proximity to the catalyst, as reactive centre. That can be fine-tuned in each case by using different voltage and current, different frequency, and change between permanent and periodic operation. The outcome of the conversion of input power into an electrical field creates a complex chemical response by formation of activated states of the molecules, with all kinds of ions, radicals and electronically, vibrationally and rotationally excited species. This complex interaction - input power to electrical plasma field to excited chemical species to reaction output - determines the energy efficiency finally.

Overall, results of the NTP-assisted synthesis processes would be influenced by the exact plasma conditions and the number of surface sites available. However, it has previously been shown that this model is able to reproduce realistic values [40]. Similarly, the values obtained in the present study, both in terms of concentration and energy cost, are in acceptable agreement with literature [56]. However, we acknowledge that although our calculated energy costs of 3,000–6,000 GJ/t NH_3 (i.e., 0.5–1.2 g-NH_3/kWh in terms of energy yield) are low compared to the state-of-the-art, still lower values are also reported in literature [27]. The highest energy efficiency was reached by Kim et al. [26,56] who obtained an energy cost of 1.5 MJ/mol NH_3 (i.e., ca. 95 GJ/t NH_3) by using a Ru catalyst promoted by Mg on a Al_2O_3 support. Unfortunately, we can currently not capture the effect of promoters in our model due to the lack of kinetic data. Furthermore, their obtained NH_3 concentration was only 0.2 mol% [56]. Compared to Rouwenhorst *et al.* and Patil *et al.* the same order of magnitude is predicted for the NH_3 concentration, as well as the same global trend for low gas temperatures (up to approximately 300 °C) [39,44]. However, we acknowledge that the specific plasma conditions are different and thus, a direct comparison is not possible.

It should be noted that the energy consumption of DBD plasmas for NH_3 synthesis is quite high. This is also true for other gas conversion applications, such as CO_2 conversion [18] and NO_x production [76] and it is attributed to the reduced electric field, which is the ratio of the electric field over the gas number density. This value is quite high for DBD plasmas (order of 200 Td or more, where 1 Td = 10^{-21} V m2), while it is typically around 50 – 100 Td in microwave, gliding arc, and atmospheric pressure glow discharges. The latter are called 'warm plasmas', as they operate at somewhat higher temperatures as well (up to a few 1000 K). The lower reduced electric field in these plasmas gives rise to electron energies in the order of 0.5–1 eV, which is ideal for electron impact vibrational excitation, known as the most efficient dissociation mechanism for N_2 (and also CO_2) molecules [76], while in DBD plasmas the reduced electric field creates higher electron energies (1 – 3 eV), mainly causing electron impact electronic excitation and ionization. These give rise to less efficient dissociation channels, explaining the lower energy efficiency of DBD plasmas. In addition, the dissociation in warm plasmas can proceed by thermal chemistry as well, with the reaction rates increasing with temperature. Finally, as demonstrated by van 't Veer et al. [41], the NH_3 produced is also partially decomposed inside the DBD plasma, more specifically inside the microdischarges, which is also responsible for the low production yield and energy efficiency. Therefore, it may be that NH_3 production in warm plasmas is more energy-efficient, although it is an exothermic process, which theoretically would benefit from low temperature, at least if the activation energy can be overcome by reactive plasma species. If the energy efficiency of plasma-based NH_3 production were higher, this would improve the overall metrics of our integrated process, but before drawing conclusions, it would need to be investigated.

What definitely has been demonstrated already in recent years is that plasma-based NO_x production is much more energy-efficient in warm plasmas than in DBD plasmas. Rouwenhorst et al. [30] made an extensive literature overview of NO_x production rates and energy cost in various plasma types, showing that plasma reactors operating at atmospheric pressure typically produce NO_x at concentrations in the percentage range with an energy cost in a very wide range, from 2.4 to 1,700 MJ/mol. Since this review paper was published, even higher NO_x concentrations and lower energy costs were reported. Indeed, a rotating gliding arc plasma could provide record-high NO_x yields up to 5.5 % for an energy cost of 2.4 MJ/mol [77], and these results could be further improved (i.e., enhanced NO_x yield by 10 % and reduction in energy cost by 23 %) by placing a specific nozzle (so-called 'effusion nozzle') at the end of the plasma reactor, which acts as efficient heat sink, and causes fast quenching of the gas after reaction, thereby preventing the decomposition of the produced NO_x back into N_2 and O_2 [78]. Another plasma type, i.e., an atmospheric pressure microwave plasma yielded the highest NO_x production rate of 0.77 L/min, for a fairly high NO_x yield of 3.8 % and an energy cost as low as 2.0 MJ/mol, in an electrodeless design, hence causing no risk of electrode damage, and thus being very promising for long-term operation, and it also revealed the promising potential of up-scaling [79]. Finally, a pulsed plasma jet demonstrated the lowest energy cost reported to-date, of 0.42 MJ/mol, almost approaching the theoretical limit of 0.2 MJ/mol, albeit for a very low NO_x yield (<0.1 %) [31]. This superior performance in terms of energy cost is ascribed to the pulsed regime, causing clear vibrational-translational non-equilibrium. Note that microwave plasmas at reduced pressure (0.01 – 0.07 bar) also produce NO_x at low energy cost [80–82], but for a fair comparison, the energy requirements to reduce the pressure and for cooling at low pressure should be added.

In the process PNOCRA, recently proposed by Hollevoet et al. [29,32], the plasma-produced NO_x was converted on a downstream Lean NO_x Trap. Based on the record-low energy cost of 0.42 MJ/mol NO_x produced in the pulsed plasma jet, this yields a total energy cost of ca. 2.1 MJ/mol for NH_3 production, making PNOCRA the least energy-

consuming small-scale NH_3 production process at mild conditions demonstrated so far. This is much lower than the values of 50–100 MJ/mol obtained in DBD plasma (cf. Fig. 4), showing that there are several possibilities for making plasma-based NH_3 production more efficient, and thus showing promise for our metrics as well.

3.3. Economic assessment of the HTP-NTP heat integration

3.3.1. Post-HTP-NTP separation of CO as a key link for the integrated process

In our vision of the thermally integrated HTP-NTP process, we like to include biomethane (biogas) besides NG to widen the scope of feeds and supply chain, as motivated in section 3.1. Sarafraz et al. [36] previously proposed to use a separation system to remove CO_2 in the biomethane feed to have a CH_4 100 wt% input to the HTP unit. Yet, there are also arguments to conduct separation after the HTP unit, such as using it standalone to produce syngas (H_2 and CO) or to valorise the CO in another way. Then, H_2 and CO are produced via the high-temperature plasma.

Yet if using it for the process proposed here, the CO might be detrimental to the consecutive ammonia NTP process and its catalyst. Therefore, we propose a post-HTP separation process of CO from H_2, which can withstand the high temperature of the HTP effluent stream. We consider those methods and discuss now their suitability for our problem. One option is the water–gas shift reaction. Here, H_2-rich gas is passed over one or more water–gas shift converters where CO reacts with steam to produce H_2 and CO_2, and then they can be separated using a membrane. However, 1–2 vol% of CO is inevitably contained in the hydrogen after the CO shift reaction [83]. Another CO removal method is to separate hydrogen through a Pd–Ag membrane. However, this method requires expensive membranes and a high-pressure differential between both sides of the membrane at high temperatures [83]. Another established approach for CO removal is the selective oxidation of CO by adding air in the presence of H_2. This method likely will not work at the temperatures foreseen for our process, and additionally has safety risks, which will become higher at the temperatures of our process [84–86]. In addition, the methanation technique is known for the complete removal of CO in hydrogen-rich gas streams over supported metal catalysts [83]. It even has the additional benefit to produce CH_4, which can be recycled into the feed. Methanation of CO is deemed to be feasible under our process conditions and thus was selected.

Accordingly, we considered the post-treatment of the H_2/CO stream by methanation of CO into CH_4 over supported nickel catalyst at temperatures over 300 °C at atmospheric pressure, which can be run at complete conversion [83]. In this sense, due to the high temperature of the H_2/CO stream, the CO reduction can be performed without additional heating. The investment costs for this H_2/CO post-treatment unit were estimated based on Outotec GmbH [73], which reported a cost rate of 130 €/kW for a 110 MW (of CH_4 output) unit. Since in our case the methanator only converts the CO content and a fraction of H_2 into a small quantity of CH_4, and in order not to underestimate the equipment cost, we calculated the need of a 44 MW methanation unit assuming complete conversion of the H_2-rich gas input flow into CH_4, and considering a 55 % chemical energy conversion efficiency [73]. This methanator would cost about 236 $/kW, i.e., an investment of 10.3 million US$.

3.3.2. Cost comparison of thermally integrated HTP-NTP and non-integrated HTP-NTP

As presented in Fig. 4, the highest energy cost benefits are achieved by performing the NTP-assisted NH_3 synthesis at temperatures of about 300 °C, which can be obtained from the heat generated in the HTP process. In this regard, we compare in Fig. 7 the final NH_3 production costs of this integrated plant (NTP reactor consumption = 3,300 GJ/t NH_3, i.e., 1.1 g NH_3/kWh yield) with a non-integrated plant (NTP reactor consumption = 4,300 GJ/t NH_3, i.e., 0.8 g NH_3/kWh yield at room temperature). In addition, to benchmark this proposal against other alternative pathways, we also estimated the production costs for the NTP-assisted synthesis supplied by H_2 produced via alkaline electrolyser (stand-alone NTP).

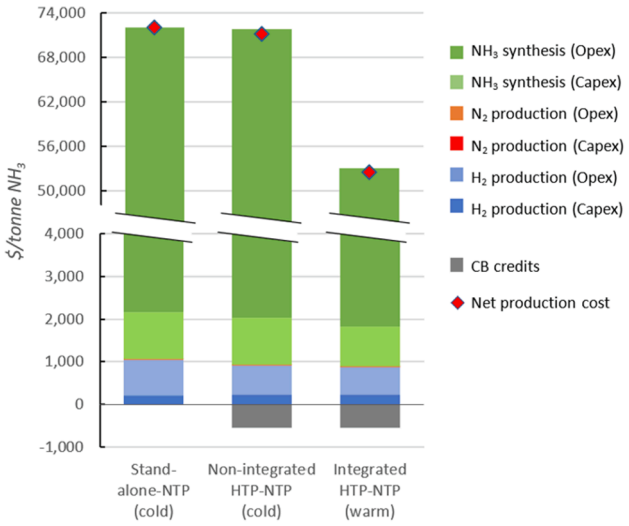

Fig. 7. Production cost breakdown of stand-alone NTP (cold), non-integrated HTP-NTP (cold), and integrated-HTP-NTP (warm) NH_3 synthesis pathways. NG price: 4 $/MMBTU; Electricity price: 0.05 $/kWh; Carbon black sale price: 1,000 $/t. Note: Red symbols in each column correspond to the net production costs (Total production costs – credits). Detailed costs are presented in Tables S1 - S12 in the Supplementary Material file.

Fig. 7 demonstrates the economic benefits of the proposed integrated HTP-NTP plant, which achieves an NH_3 production cost of 52,492 $/t NH_3, corresponding to cost reductions of about 26 % and 27 % compared to the low-temperature NTP NH_3 synthesis supplied by HTP or electrolysers units, respectively.

However, in these scenarios, about 98 % of the net production costs correspond to the operation of the NH_3 synthesis process, of which 90 % amount to the electricity consumption. Even the proposed acceleration of the reaction rate, as given by the plasma chemical kinetic simulations in section 3.2, still leads to a far too low NTP energy yield of 1.1 g NH_3/kWh. It should be noted that the CB credits reduce these costs for the integrated HTP-NTP pathways, but they are not sufficient to compensate for the fact that the NTP costs are ill defined.

3.3.3. Cost comparison of thermally integrated HTP-NTP with future scenarios on energy efficiency

Since most of the costs are related to the low energy yield in the NTP reactor, to better judge the value of our proposed thermal integration concept, we performed a sensitivity analysis by considering literature values for a more energy-efficient NTP process; having the same commercial viability as the HTP process has today. In this regard, we evaluated the economic performance of a plant with the highest energy yield obtained in literature of 35.7 g NH_3/kWh, also obtained at 1 bar and 300 °C [26], which reduces the energy consumption in the reactor to 28 kWh/kg NH_3. On the other hand, we evaluated a future scenario for a potential energy yield of 900 g NH_3/kWh stated by Rouwenhorst et al. [25,56], which corresponds to an expected energy consumption in the reactor of 4 GJ/t NH_3, i.e., 1.11 kWh/kg NH_3.

In this way, the net production costs for the integrated HTP-NTP process in the scenario of the highest energy yield obtained in literature are reduced to 2,061 $/t NH_3 (see Fig. 8). For this scenario, about 88.4 % of the costs are due to the NTP section, while 10.8 % is in the HTP section and 0.8 % in the N_2 production section. In the scenario of the theoretical maximum NTP energy yield, the net production cost would be reduced to 452 $/t NH_3. In this future scenario, the NTP section

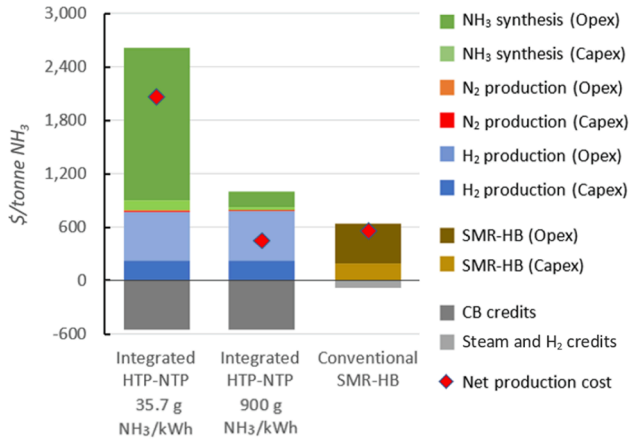

Fig. 8. Production cost breakdown of integrated HTP-NTP NH_3 synthesis, considering different NTP energy yields, and conventional SMR-HB synthesis route. NG price: 4 $/MMBTU; Electricity price: 0.05 $/kWh; Carbon black sale price: 1,000 $/t. Note: Red symbols in each column correspond to the net production costs (Total production costs – credits). Detailed costs are presented in Tables S13 - S24 in the Supplementary Material file.

would still have important participation of 45 % of the net production costs. The HTP section participates with 51 % of the net production cost. However, if the CB credits were not considered, the net production costs would increase to 1,001 $/t NH_3 and the HTP section would participate with 78 % of the net production costs. In this sense, if CB credits are considered in the economic assessment, the proposed integrated HTP-NTP plant in the scenario of the best energy yield for the NTP-assisted NH_3 synthesis would obtain lower costs than the small-scale conventional SMR-HB plant, which we estimated as 584 $/t NH_3. Similarly, we estimated for a world-scale 1-million-tonne NH_3/year plant costs about 336 $/t NH_3. As evidence of the accuracy of our calculations, we like to refer to the price of world-scale produced ammonia, which has historically fluctuated around $300–400/t NH_3.

Moreover, we take one step further in assuming optimistic NTP energy efficiencies in order to reach a judgment on the economic value of our proposed thermal integration of HTP and NTP. In a scenario-wise manner and based on literature, we conducted an exploratory analysis with respect to a set of NH_3 synthesis energy yield values, see Fig. 9.

The three data points in Fig. 9 (left chart) consider energy yields of 1.1, 35.7, and 900 g NH_3/kWh, which correspond to our simulation result, the maximum value reported in literature [26], and the potential energy yield [55], respectively. The grey dashed line in Fig. 9 (right chart) represents the estimated production cost from the small-scale SMR-HB plant. From this perspective, the proposed integrated HTP-NTP plant would produce NH_3 with lower costs than the conventional route when the NTP reactor reaches energy yields over 310 g NH_3/kWh. In this scenario, if we assume that also the energy yield of the HTP reactor is improved at the same extent (i.e., from 40.5 to 352 g H_2/kWh), as well as assuming a slight reduction in the electricity costs, the proposed HTP-NTP plant for distributed production would reach production costs similar to those obtained by large centralized SMR-HB plants, as shown in Fig. 10. In addition, we can see that the NH_3 production costs are not too sensitive to the HTP energy yield because the HTP process is not as electricity-intensive as the NTP-assisted NH_3 synthesis. In this sense, further efforts should focus on the NTP section.

From these analyses, we see that the greater the electrical efficiency of the reactors, the greater the share of the HTP section to the total production costs, as can be seen in Fig. 8 for the scenario of the most efficient NTP process, where operating costs of H_2 production (in light blue) are the most relevant. The methane input is a parameter that greatly affects the NH_3 production cost, which can be a concern given the recent observed volatility of NG prices. In Australia, NG has reached prices near 8 US$/MMBTU [87]. In case of using biomethane, although it is produced from local raw materials, its price would be influenced by the opportunity cost when biomethane is from a third-party supplier. This situation would be similar for renewable-based electricity because prices of grid electricity have also increased in several regions, although to a lesser extent than the NG price [88]. However, although methane and electricity prices represent relevant operating costs in the HTP section, another key parameter that affects this section the most is the sale price of CB credits (in grey in Fig. 8), which would help offset input costs because CB price has also been rising. For these reasons, it was pertinent to perform a sensitivity analysis for these parameters, as presented in Fig. 11.

In Fig. 11, the defined NTP energy yield was chosen to consider the point in which the conventional and the proposed plants match (584 $/t NH_3) in the scenario presented in Fig. 9 (electricity: 0.05 $/kWh; NG: 4

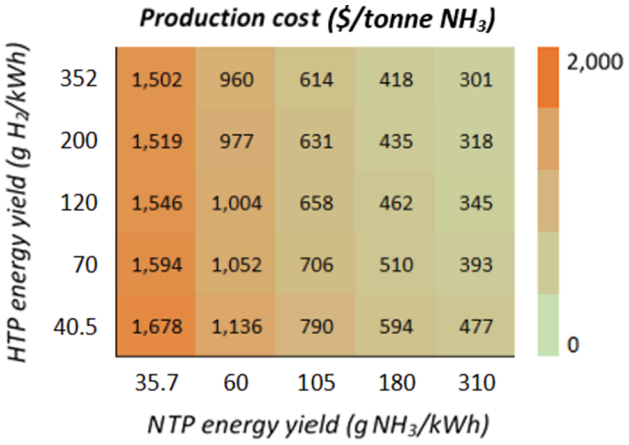

Fig. 10. Effect of HTP and NTP energy yields on NH_3 production cost (expressed in $/tonne NH_3). Electricity price: 0.04 $/kWh; NG: 4 $/MMBTU; CB sale price: 1,000 $/t. Note: values in both axes are increased by 70% each time.

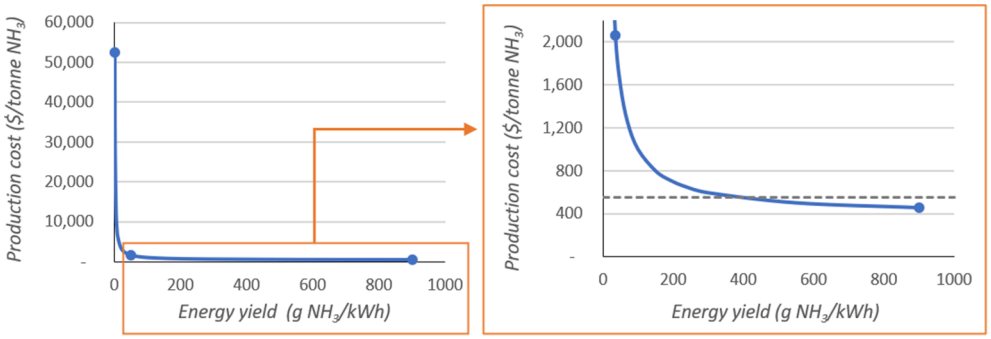

Fig. 9. Effect of NTP energy yield on NH_3 production cost. Electricity price: 0.05 $/kWh; NG: 4 $/MMBTU; CB sale price: 1,000 $/t.

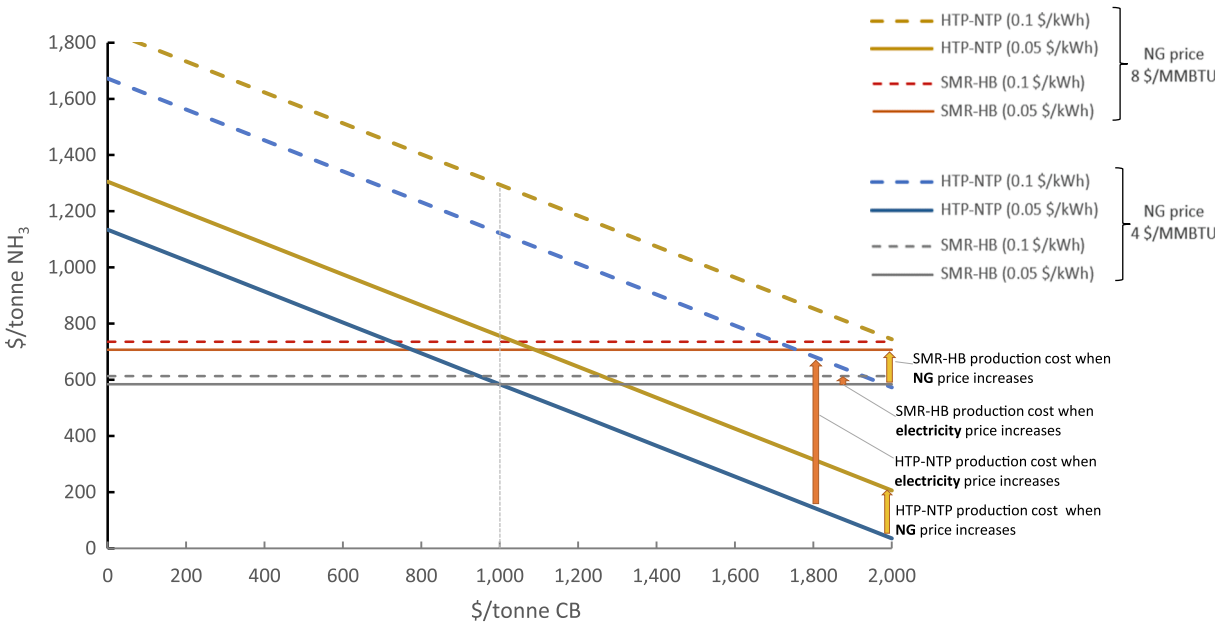

Fig. 11. Effect of prices of NG, electricity, and CB on the NH_3 production costs for the integrated HTP-NTP and SMR-HB plants. Note: NTP energy yield 310 g NH_3/kWh at 1.0 mol% NH_3.

$/MMBTU; CB: 1,000 $/t). Since the HTP-NTP plant depends on only few inputs in comparison to SMR-HB plants (as shown in Table 1), it can be seen in Fig. 11 that the HTP-NTP plant is slightly more sensitive to variations in the NG prices and highly sensitive to variations in the electricity prices. For example, when the NG price doubles, the NH_3 cost increases 171 $/t NH_3 in the HTP-NTP plant and 123 $/t NH_3 in the SMR-HB plant. When the electricity prices doubles, the NH_3 cost increases 538 $/t NH_3 in the HTP-NTP plant and only 28 $/t NH_3 in the SMR-HB plant. On the other hand, CB prices affect the NH_3 cost in the HTP-NTP plant to a higher extent than electricity prices, e.g., increasing by 550 $/t NH_3 when CB prices double from 1,000 to 2,000 $/t CB, which could reduce the NH_3 production costs to zero. In the same way, any decrease of CB prices can proportionally rise the NH_3 costs, making the HTP-NTP plant highly dependent of this external factor. Yet, historical CB prices have not shown the high volatility as NG and electricity prices, which would suggest that these plants could keep a stable NH_3 production cost by integrating self-managed renewable energy generation systems.

3.3.4. *Cost comparison of thermally integrated HTP-NTP with pre- and post-separation*

Since both fossil NG and biomethane contain impurities such as CO_2 which generates the presence of CO in the outlet stream, different production costs could result due to their diverse equipment and energy requirements. For a cost comparison, we analysed case 1 in which the feed gas consisted of 100 % CH_4, requiring a pre-treatment step to completely eliminate CO_2 in the biogas input and, at the same time, eliminating the need of the post-treatment step via the methanation unit, as utilized in Fig. 1.

The most common technologies for the CO_2 removal of CH_4-rich gases are pressurized water scrubbing, amine scrubbing, pressure swing adsorption, cryogenic separation and membrane technologies [89,90]. The latter was selected because among the technologies that deliver high purity methane, membrane technologies are compact, have low energy demand and relatively lower investment costs than cryogenic separators [89,90]. In this analysis, we utilised a membrane-based separator system with a capacity of 14,472 $Nm^3.h^{-1}$, which consumes 0.3 kWh/Nm^3 [89]. This equipment would cost about 1,157 $/($Nm^3.h^{-1}$), i.e., an investment of 16.7 million US$, estimated from the reported cost of 3,600 €/($Nm^3.h^{-1}$) for a separator with a capacity of 500 $Nm^3.h^{-1}$ [89]. Detailed costs for this integrated HTP-NTP plant using methane pre-separation technology are presented in Tables S25-S28 in the Supplementary Material file.

Given that the assumed capital cost for the membrane-based separator was higher than the cost of the methanation unit, as well as it requires additional electricity consumption, the H_2 production cost from the HTP process with pre-separation increased by 20 % (i.e., from 1,214 to 1,457 $/t H_2), considering a NG price of 4 $/MMBTU and electricity price of 0.05 $/kWh. This higher H_2 cost makes to increase the NH_3 production cost by 2.16 % (i.e., from 2,061 to 2,105 $/t NH_3), in the scenario of the 35.7 g NH_3/kWh energy yield. On the other hand, considering a biomethane price of about 11 $/MMBTU [91–93], the H_2 produced in the HTP process with pre-separation was 156 % higher than the HTP process with post-separation (i.e., 3,103 $/t H_2). In this case, the NH_3 production cost increased by 17 % (i.e., 2,405 $/t NH_3). In both cases with different feedstock prices and separation technologies, this HTP process achieves lower H_2 cost than other alternative routes, such as electrolyser-based systems with costs over 5,000 $/t H_2, mainly due to the contribution of CB credits.

In the scenario of integrating the HTP process (40.5 g H_2/kWh) with the NTP process (310 g NH_3/kWh), the H_2 cost increase by using pre-separation technology would hardly affect the NH_3 final cost, achieving rates of 629 $/t NH_3 (8 % higher than using post-separation technology). On the other hand, the HTP section supplied by biomethane and using pre-separation technology would achieve costs of 929 $/t NH_3.

3.4. *Environmental assessment of the HTP-NTP heat integration*

Following the same scenarios for the base and sensitivity analyses on the different NH_3 synthesis pathways presented in the TEA section, we have estimated the life cycle carbon emissions to produce each tonne of NH_3 from cradle-to-gate, as shown in Fig. 12.

Since the electricity used for the LCA in Fig. 12 is from the Australian grid, for which about 87 % is produced from fossil energy sources [68,94], the higher consumption of electricity, the higher the carbon emissions. For this reason, the emission rates of the evaluated pathways have a similar trend to those observed in the costs analysis. However, in comparison to the emission rate for the conventional SMR-HB pathway of 2.1 t CO_2 eq/t NH_3 [61], the proposed integrated HTP-NTP plant

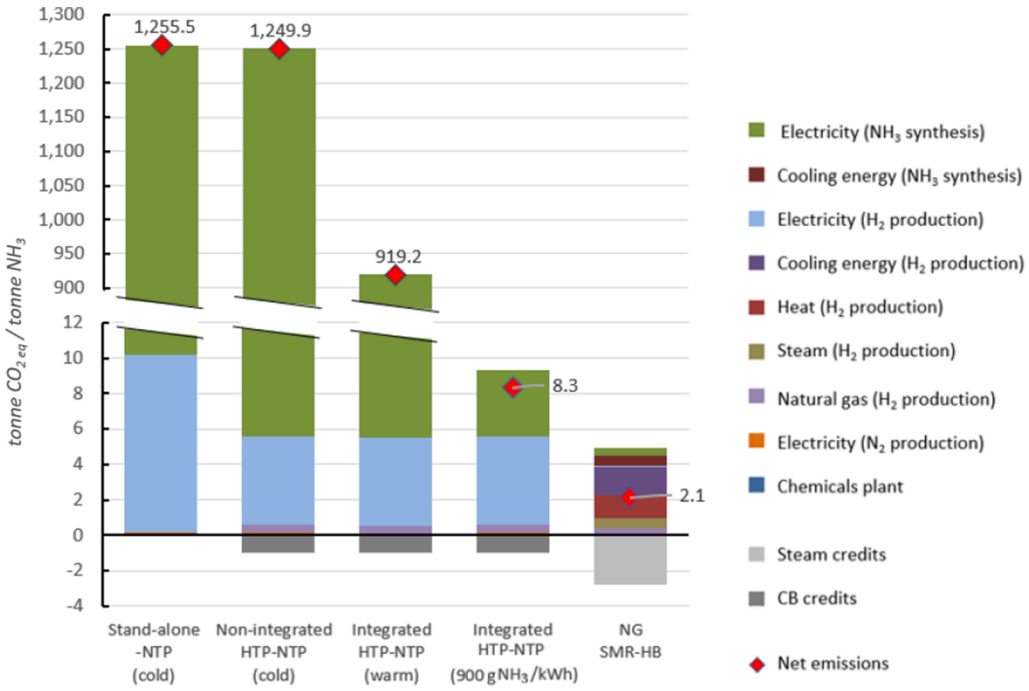

Fig. 12. Global warming potential of stand-alone NTP (cold: 0.8 g NH_3/kWh), non-integrated HTP-NTP (cold: 0.8 g NH_3/kWh), integrated-HTP-NTP both (warm: 1.1 g NH_3/kWh) and (expected: 900 g NH_3/kWh), and conventional SMR-HB. All pathways use electricity from the Australian grid. Inputs with shares lower than 1 % of the total impact, such as water, catalysts, and other by-products than steam (from the SMR-HB plant), were excluded from this chart. Note: Red symbols in each column correspond to the net carbon emissions.

would never be environmentally friendly if electricity from fossil sources is utilised. In this sense, it is evident that the future of commercial applications of NTP-assisted NH_3 synthesis plants would be strongly linked to the availability of clean and affordable energy sources.

Nevertheless, as stated by Fasihi et al. [58] and Squadrito et al. [52], electricity costs from wind and solar photovoltaic sources have been falling, offering the possibility to produce cost-effective green hydrogen in the next decades and, therefore, opening the door to affordable green ammonia production. In this way, renewable energy scenarios for the stand-alone NTP (cold) and the integrated HTP-NTP plants with different NTP energy yields, supplied with biogas from biogenic resources (i.e., biowaste), and using photovoltaic or wind electricity, are presented in Fig. 13.

In Fig. 13, when using photovoltaic electricity, the proposed integrated HTP-NTP process would reduce by half the net emissions (i.e., 1.2 t CO_2 eq/t NH_3) in comparison to the conventional SMR-HB pathway, when assuming the maximum NTP energy yield reported so far. In the scenario of wind energy, the carbon emission balance is

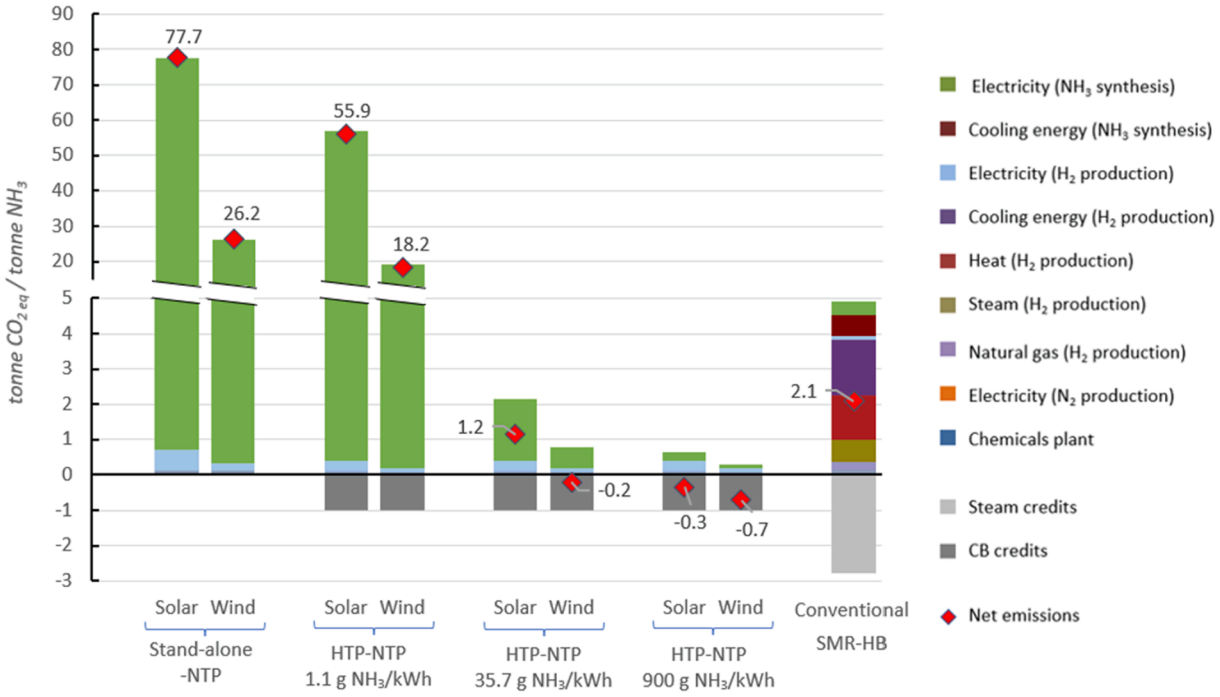

Fig. 13. Global warming potential of stand-alone NTP, integrated-HTP-NTP (with different NTP energy yields), and conventional SMR-HB pathways in different energy scenarios. Inputs with shares lower than 1% of the total impact, such as water, catalysts, and other by-products than steam by-products (from the SMR-HB plant), were excluded from this chart. Note: Red symbols in each column correspond to the net carbon emissions.

inverted due to the CB credits, generated by a market reduction for the traditional made CB using fossil sources.

In terms of energy consumption, the best available techniques for the SMR-HB have shown rates of 27.4 – 31.8 GJ/t NH_3 [57]. For the proposed HTP-NTP plant, only the HTP section consumes 40.6 GJ/t NH_3 from the energy content of the methane input, plus 18 GJ/t NH_3 of electricity. Hence, adding the energy consumption of the PSA unit and the NTP section in the best scenario, corresponding to 9.3 GJ/t NH_3, the total energy consumption would be around 68 GJ/t NH_3. However, considering that the CB credits would avoid the conventional CB production from crude oil, which requires 70.3 GJ/t CB, the net energy consumption of the HTP-NTP process would be around 29.3 GJ/t NH_3. In this sense, considering the NH_3 energy content of 18.6 GJ/t, the energy efficiency of both the SMR-HB and the integrated HTP-NTP process would be around 63 %.

However, in the context of LCA, the CED and CExD show better results for the alternative pathways when considering the use of renewable energies. For example, using fossil fuels and grid electricity, the CED and CExD for the SMR-HB plant were 49.8 and 53.5 GJ/t NH_3, respectively. For the best scenario of the HTP-NTP plant, the CED and CExD were 78.9 and 87.6 GJ/t NH_3, considering the CB credits. These large figures are due to the high usage of coal and lignite in power generation in Australia, energy-intensive mining sources, in thermal plants with lower energy efficiency than renewable, hydroelectric, and combined-cycle gas turbine plants. In contrast, the CED and CExD for the HTP-NTP plant supplied by photovoltaic electricity were −4.4 and −7.8 GJ/t NH_3, respectively. Similarly, when this plant is supplied by biogas and by wind energy, the CED and CExD were −9 and −11.34 GJ/t NH_3, respectively. In both solar and wind energy scenario, most of the energy and exergy contributions were due to the manufacturing of solar panels and wind turbines, but thanks to the CB credits these balances were inverted, showing a similar trend to the reduction of the carbon emissions in these alternative NH_3 production pathways.

4. Conclusions

We propose a novel integrated plasma-based NH_3 synthesis process, flexibly based on natural gas or biogas, and the innovation is a unique combination of a high-temperature plasma (HTP) and non-thermal plasma (NTP). As all carbon of the natural gas is bound in the high-value product carbon black, only a small CO_2 footprint is given at the HTP stage when using natural gas, and the process is classified as "turquoise hydrogen" manufacture [95]. In addition, we show, for the first time, that biogas can be used as feed for the HTP process. We evaluated this process from the techno-economic performance perspective as well as by anticipatory life cycle assessment focusing on the global warming potential (CO_2 footprint). We carried out process modelling simulations for H_2 synthesis from biogas using HTP, and NH_3 synthesis from H_2 using NTP.

Central to our approach is to use the hot HTP effluent stream to be entered the NTP zone without cooling down, creating a 'warm plasma'. Plasma chemical kinetics simulations, conducted for a wide range of plasma-plausible catalysts and operating temperatures, helped us to answer at which 'warm temperature' the NTP can be best operated, seen from the NTP reactor productivity side. The plasma chemical kinetics simulations indicated that an NH_3 concentration of 2.2 mol% can be attained at 302 °C on a Fe surface at an energy cost of 3,300 GJ/t NH_3.

Our cost-calculations for such optimised HTP-NTP process show, as to be expected, that with the consideration of the low energy yields of the NTP process, the whole costing is (negatively) dominated by the NTP process, and the economic benefits are hardly evident with the current NTP technology. Nevertheless, we have strong arguments to assume higher energy efficiencies, and we did this in a two-step manner, (i) based on the best experimental evidence in current literature, and (ii) trustable forecasts on future NTP energy efficiencies. With the latter, we succeeded in showing an overall near-commercial operation of our thermally integrated HTP-NTP process to yield ammonia; as possible for a small-scale plant, following our vision on distributed fertiliser production. Under such best assumptions, costs come down to 452 $/t NH_3, which are below the estimated cost for the conventional SMR-HB route at similar scales with about 584 $/t NH_3, and near to the large centralized SMR-HB with costs of about 300 $/t NH_3.

Besides that, we show the process-chemical feasibility of using biogas in the HTP process, by proposing appropriate separation technologies for the whole thermally integrated HTP-NTP process. Our process simulation results demonstrate that a higher CO_2 content in the biogas feed increases accordingly the CO concentration in the product stream, yet with minimal effect on the H_2 yield. The latter is interesting to note, since O_2 is produced, yet this burns some carbon and reduces the CB yield, rather than taking the H_2. We found that at reaction temperatures above 1200 °C the product yield remains constant. A disadvantage of using biogas in the HTP section without prior separation of CO_2 is the larger reactor volume for the same H_2 capacity as given for a pure methane feed. We also determined the costs of a biogas-based thermally integrated HTP-NTP process, which are somewhat higher than the above-given scenarios.

We strongly advocate compensating for the higher costs of the distributed green technologies with various kinds of 'credits' (carbon, soil, jobs, co-valorisation). Moreover, to avoid the effects of the volatility of NG and electricity prices, these plants might be integrated into their own renewable-based energy generation systems. We have demonstrated that the integrated HTP-NTP process with the current maximum energy yields can cut half the carbon emissions, in comparison to the conventional made NH_3, when supplied by photovoltaic electricity and biogas. Moreover, if these plants were supplied by wind power, the carbon emission balance can be inverted due to the additional avoided emissions by the production of cleaner CB co-product.

In brief, the benefits of being resilient and self-sufficient need such co-financing, and the economic opportunity is real. The conventional technology cannot account for the benefits of a community in the sense of the credits. This theoretical study predicts a far-future performance of a plasma system to manufacture ammonia. We acknowledge that the gap between todays and future performance probably will stay for longer be a road-blocker for the commercialisation of the plasma fertiliser technology. The paper, nonetheless, wants to help to solve current eminent global issues in food supply, having escalated to supply crisis situations, by providing new solutions to the fertiliser manufacture. Therefore, we assume the best future scenarios of electrical efficiency of plasma conversion. In addition, we assume the plasma-related credit-financing of co-products and reduction of carbon footprint. In addition, we propose local manufacturing of fertilisers, up to the farm site, with further benefits [96]. Admittedly, the NTP side needs to be improved nonetheless, to make this process economically viable.

CRediT authorship contribution statement

Jose Osorio-Tejada: Conceptualization, Investigation, Methodology, Writing – original draft, Writing – review & editing. **Kevin van't Veer:** Conceptualization, Investigation, Methodology, Writing – review & editing. **Nguyen Van Duc Long:** Conceptualization, Investigation, Methodology, Writing – review & editing. **Nam N. Tran:** Methodology, Writing – review & editing. **Laurent Fulcheri:** Methodology, Writing – review & editing. **Bhaskar Patil:** Methodology, Writing – review & editing. **Annemie Bogaerts:** Conceptualization, Methodology, Writing – review & editing, Supervision, Resources, Project administration, Funding acquisition. **Volker Hessel:** Conceptualization, Methodology, Writing – review & editing, Supervision, Resources, Project administration, Funding acquisition.

Declaration of Competing Interest

The authors declare the following financial interests/personal

relationships which may be considered as potential competing interests: [Volker Hessel reports financial support was provided by European Research Council.].

Data availability

Data will be made available on request.

Acknowledgements

The authors acknowledge support from the ERC Synergy Grant "Surface-COnfined fast modulated Plasma for process and Energy intensification" (SCOPE), from the European Commission, with Grant No. 810182.

Appendix A. Supplementary material

Supplementary data to this article can be found online at https://doi.org/10.1016/j.enconman.2022.116095.

References

[1] Arnaiz del Pozo C, Cloete S, Jiménez Álvaro Á. Techno-economic assessment of long-term methanol production from natural gas and renewables. Energy Convers Manag 2022;266:115785. 10.1016/J.ENCONMAN.2022.115785.
[2] Bai W, Qiao Y, Wang C, Li H, Zhang X, Zhang C, et al. Comprehensive assessments of a novel aluminum-fueled energy storage system. Energy Convers Manag 2022; 266:115615. https://doi.org/10.1016/J.ENCONMAN.2022.115615.
[3] Incer-Valverde J, Patiño-Arévalo LJ, Tsatsaronis G, Morosuk T. Hydrogen-driven Power-to-X: State of the art and multicriteria evaluation of a study case. Energy Convers Manag 2022;266:115814. https://doi.org/10.1016/J.ENCONMAN.2022.115814.
[4] Sarafraz MM, Tran NN, Pourali N, Rebrov EV, Hessel V. Thermodynamic potential of a novel plasma-assisted sustainable process for co-production of ammonia and hydrogen with liquid metals. Energy Convers Manag 2020;210:112709. https://doi.org/10.1016/J.ENCONMAN.2020.112709.
[5] Yapicioglu A, Dincer I. A review on clean ammonia as a potential fuel for power generators. Renew Sustain Energy Rev 2019;103:96–108. https://doi.org/10.1016/J.RSER.2018.12.023.
[6] Roberts TL. The role of fertilizer in growing the world's food. Better Crop 2009;93:12–5.
[7] UN. Summary of the seventh high-level meeting of the Development Cooperation Forum. Development Cooperation for the Decade of Action Reduce risk. Enable recovery. Build resilience. 2021.
[8] Hannam P. What is urea and AdBlue, and why does a worldwide shortage threaten Australia's supply chain? Guard 2021.
[9] Baqaee D, Farhi E. Nonlinear Production Networks with an Application to the Covid-19 Crisis. Cambridge 2020.
[10] Sarafraz MM, Christo FC, Tran NN, Fulcheri L, Hessel V. Thermal plasma-aided chemical looping carbon dioxide dissociation for fuel production from aluminium particles. Energy Convers Manage 2022;257:115413. https://doi.org/10.1016/J.ENCONMAN.2022.115413.
[11] Fulcheri L, Schwob Y. From methane to hydrogen, carbon black and water. Int J Hydrogen Energy 1995;20:197–202. https://doi.org/10.1016/0360-3199(94)E0022-Q.
[12] Li D, Rohani V, Fabry F, Parakkulam Ramaswamy A, Sennour M, Fulcheri L. Direct conversion of CO2 and CH4 into liquid chemicals by plasma-catalysis. Appl Catal B Environ 2020;261:118228. https://doi.org/10.1016/J.APCATB.2019.118228.
[13] Gautier M, Rohani V, Fulcheri L. Direct decarbonization of methane by thermal plasma for the production of hydrogen and high value-added carbon black. Int J Hydrogen Energy 2017;42:28140–56. https://doi.org/10.1016/J.IJHYDENE.2017.09.021.
[14] Hrabovsky M, Hlina M, Kopecky V, Maslani A, Krenek P, Serov A, et al. Steam Plasma Methane Reforming for Hydrogen Production. Plasma Chem Plasma Process 2018;38:743–58. https://doi.org/10.1007/s11090-018-9891-5.
[15] Tamošiūnas A, Valatkevičius P, Gimžauskaitė D, Valinčius V, Jeguirim M. Glycerol steam reforming for hydrogen and synthesis gas production. Int J Hydrogen Energy 2017;42:12896–904. https://doi.org/10.1016/j.ijhydene.2016.12.071.
[16] Lian HY, Li XS, Liu JL, Zhu AM. Methanol steam reforming by heat-insulated warm plasma catalysis for efficient hydrogen production. Catal Today 2019;337:76–82. https://doi.org/10.1016/j.cattod.2019.03.068.
[17] Chun YN, Kim SC. Production of hydrogen-rich gas from methane by thermal plasma reform. J Air Waste Manag Assoc 2007;57:1447–51. https://doi.org/10.3155/1047-3289.57.12.1447.
[18] Snoeckx R, Bogaerts A. Plasma technology-a novel solution for CO2 conversion? Chem Soc Rev 2017;46:5805–63. https://doi.org/10.1039/c6cs00066e.
[19] Shah J, Wang W, Bogaerts A, Carreon ML. Ammonia synthesis by radio frequency plasma catalysis: revealing the underlying mechanisms. ACS Appl Energy Mater 2018;1:4824–39. https://doi.org/10.1021/acsaem.8b00898.
[20] Xie D, Sun Y, Zhu T, Fan X, Hong X, Yang W. Ammonia synthesis and by-product formation from H2O, H2 and N2 by dielectric barrier discharge combined with an Ru/Al2O3 catalyst. RSC Adv 2016;6:105338–46. https://doi.org/10.1039/C6RA21351K.
[21] Wang Y, Craven M, Yu X, Ding J, Bryant P, Huang J, et al. Plasma-enhanced catalytic synthesis of ammonia over a Ni/Al2O3 catalyst at near-room temperature: insights into the importance of the catalyst surface on the reaction mechanism. ACS Catal 2019;9:10780–93. https://doi.org/10.1021/acscatal.9b02538.
[22] Sugiyama K, Akazawa K, Oshima M, Miura H, Matsuda T, Nomura O. Ammonia synthesis by means of plasma over MgO catalyst. Plasma Chem Plasma Process 1986;6:179–93.
[23] Mingdong B, Xiyao B, Zhitao Z. Synthesis of Ammonia in a Strong Electric Field Discharge at Ambient Pressure 2000;20:511–20.
[24] Patil BS, S. R. van Kaathoven A, Peeters F, Cherkasov N, Wang Q, Lang J, et al. Deciphering the synergy between plasma and catalyst support for ammonia synthesis in a packed DBD reactor. J Phys D Appl Phys 2020;53:1–13. 10.1088/1361-6463/ab6a36.
[25] Rouwenhorst KHR, Engelmann Y, Van 't Veer K, Postma RS, Bogaerts A, Lefferts L. Plasma-driven catalysis: Green ammonia synthesis with intermittent electricity. Green Chem 2020;22:6258–87. 10.1039/d0gc02058c.
[26] Kim HH, Teramoto Y, Ogata A, Takagi H, Nanba T. Atmospheric-pressure nonthermal plasma synthesis of ammonia over ruthenium catalysts. Plasma Process Polym 2017;14. https://doi.org/10.1002/ppap.201600157.
[27] Rouwenhorst KHR, Kim H-H, Lefferts L. Vibrationally excited activation of N2 in plasma-enhanced catalytic ammonia synthesis: a kinetic analysis. ACS Sustain Chem Eng 2019;7:17515–22. https://doi.org/10.1021/acssuschemeng.9b04997.
[28] Shah J, Harrison J, Carreon M. Ammonia plasma-catalytic synthesis using low melting point alloys. Catalysts 2018;8:437. https://doi.org/10.3390/catal8100437.
[29] Hollevoet L, Jardali F, Gorbanev Y, Creel J, Bogaerts A, Martens JA. Towards green ammonia synthesis through plasma-driven nitrogen oxidation and catalytic reduction. Angew Chemie - Int Ed 2020;59:23825–9. https://doi.org/10.1002/anie.202011676.
[30] Rouwenhorst KHR, Jardali F, Bogaerts A, Lefferts L. From the Birkeland-Eyde process towards energy-efficient plasma-based NO: Xsynthesis: a techno-economic analysis. Energy Environ Sci 2021;14:2520–34. https://doi.org/10.1039/d0ee03763j.
[31] Vervloessem E, Gorbanev Y, Nikiforov A, De Geyter N, Bogaerts A. Sustainable NOx production from air in pulsed plasma: elucidating the chemistry behind the low energy consumption. Green Chem 2022;24:916–29. https://doi.org/10.1039/d1gc02762j.
[32] Hollevoet L, Vervloessem E, Gorbanev Y, Nikiforov A, De Geyter N, Bogaerts A, et al. Energy-Efficient Small-Scale Ammonia Synthesis Process with Plasma-enabled Nitrogen Oxidation and Catalytic Reduction of Adsorbed NOx. ChemSusChem 2022;e202102526. 10.1002/cssc.202102526.
[33] Aspen Plus. Aspen Technology, Inc. - USA 2020.
[34] van 't Veer K, Reniers F, Bogaerts A. Zero-dimensional modelling of unpacked and packed bed dielectric barrier discharges: The role of vibrational kinetics in ammonia synthesis. Plasma Sources Sci Technol 2020;29:045020.
[35] Pancheshnyi, S.; Eismann, B.; Hagelaar, G. J. M.; Pitchford LC. Computer code ZDPlasKin. n.d.
[36] Sarafraz MM, Tran NN, Nguyen H, Fulcheri L, Burton R, Wadewitz P, et al. Tri-fold process integration leveraging high- and low-temperature plasmas: From biomass to fertilizers with local energy and for local use. J Adv Manuf Process 2021;3:1–21. https://doi.org/10.1002/amp2.10081.
[37] Monolith Inc. Monolith To Build Anhydrous Ammonia Plant Near Hallam To Use Hydrogen 2020. https://monolith-corp.com/news/monolith-to-build-anhydrous-ammonia-plant-near-hallam-to-use-hydrogen (accessed September 10, 2021).
[38] Peeters F, Butterworth T. Electrical diagnostics of dielectric barrier discharges. Atmos Press Plasma—from Diagnostics to Appl 2018.
[39] Rouwenhorst KHR, Burbach HGB, Vogel DW, Núñez Paulí J, Geerdink B, Lefferts L. Plasma-catalytic ammonia synthesis beyond thermal equilibrium on Ru-based catalysts in non-thermal plasma. Catal Sci Technol 2021;11:2834–43. https://doi.org/10.1039/D0CY02189J.
[40] van 't Veer K, van Alphen S, Remy A, Gorbanev Y, Geyter N De, Snyders R, et al. Spatially and temporally non-uniform plasmas: microdischarges from the perspective of molecules in a packed bed plasma reactor. J Phys D Appl Phys 2021; 54:174002. 10.1088/1361-6463/abe15b.
[41] van 't Veer K, Engelmann Y, Reniers F, Bogaerts A. Plasma-Catalytic Ammonia Synthesis in a DBD Plasma: Role of Microdischarges and Their Afterglows. J Phys Chem C 2020;124:22871–83. 10.1021/acs.jpcc.0c05110.
[42] Fogler HS. Elements of chemical reaction engineering. Third edition. Upper Saddle River, N.J. : Prentice Hall PTR, [1999] ©1999; 1999.
[43] Engelmann Y, Van'T Veer K, Gorbanev Y, Neyts EC, Schneider WF, Bogaerts A. Plasma Catalysis for Ammonia Synthesis: A Microkinetic Modeling Study on the Contributions of Eley-Rideal Reactions. ACS Sustain Chem Eng 2021;9:13151–63. 10.1021/acssuschemeng.1c02713.
[44] Patil BS, Cherkasov N, Srinath NV, Lang J, Ibhadon AO, Wang Q, et al. The role of heterogeneous catalysts in the plasma-catalytic ammonia synthesis. Catal Today 2021;362:2–10. https://doi.org/10.1016/j.cattod.2020.06.074.
[45] Anastasopoulou A, Keijzer R, Patil B, Lang J, van Rooij G, Hessel V. Environmental impact assessment of plasma-assisted and conventional ammonia synthesis routes. J Ind Ecol 2020;24:1171–85. https://doi.org/10.1111/jiec.12996.
[46] Anastasopoulou A, Keijzer R, Butala S, Lang J, Van Rooij G, Hessel V. Eco-efficiency analysis of plasma-assisted nitrogen fixation. J Phys D Appl Phys 2020; 53. https://doi.org/10.1088/1361-6463/ab71a8.

[47] da Costa Labanca AR. Carbon black and hydrogen production process analysis. Int J Hydrogen Energy 2020;45:25698–707. https://doi.org/10.1016/j.ijhydene.2020.03.081.
[48] Dobslaw D, Schulz A, Helbich S, Dobslaw C, Engesser KH. VOC removal and odor abatement by a low-cost plasma enhanced biotrickling filter process. J Environ Chem Eng 2017;5:5501–11. https://doi.org/10.1016/J.JECE.2017.10.015.
[49] NREL. H2A: Hydrogen Analysis Production Models | Hydrogen and Fuel Cells | NREL. Curr Cent Hydrog Prod from Polym Electrolyte Membr Electrolysis Version 32018 2019. https://www.nrel.gov/hydrogen/h2a-production-models.html (accessed September 10, 2021).
[50] Kohl AL, Nielsen RB. Membrane Permeation Processes. Gas Purif., Gulf Professional Publishing; 1997, p. 1238–95. 10.1016/B978-088415220-0/50015-X.
[51] Jenkins S. CE Plant Cost Index (CEPCI) update 2021. https://www.chemengonline.com/2021-cepci-updates-june-prelim-and-may-final (accessed September 10, 2021).
[52] Squadrito G, Nicita A, Maggio G. A size-dependent financial evaluation of green hydrogen-oxygen co-production. Renew Energy 2021;163:2165–77. https://doi.org/10.1016/J.RENENE.2020.10.115.
[53] Demirhan CD, Tso WW, Powell JB, Pistikopoulos EN. Sustainable ammonia production through process synthesis and global optimization. AIChE J 2019;65. https://doi.org/10.1002/aic.16498.
[54] Whitesides RW. Process Equipment Cost Estimating by Ratio and Proportion. Course Notes: PDH Course G; 2012. p. 8.
[55] Rouwenhorst KHR, Krzywda PM, Benes NE, Mul G, Lefferts L. Ammonia production technologies. Techno-Economic Challenges Green Ammon as an Energy Vector 2021:41–83. https://doi.org/10.1016/B978-0-12-820560-0.00004-7.
[56] Rouwenhorst KHR, Lefferts L. Feasibility study of plasma-catalytic ammonia synthesis for energy storage applications. Catalysts 2020;10. https://doi.org/10.3390/catal10090999.
[57] Smith C, Hill AK, Torrente-Murciano L. Current and future role of Haber-Bosch ammonia in a carbon-free energy landscape †. Energy Environ Sci 2020;13:331. https://doi.org/10.1039/c9ee02873k.
[58] Fasihi M, Weiss R, Savolainen J, Breyer C. Global potential of green ammonia based on hybrid PV-wind power plants. Appl Energy 2021;294:116170. https://doi.org/10.1016/j.apenergy.2020.116170.
[59] Ulrich GD, Vasudevan PT. How to estimate utility costs. Chem Eng 2006;113.
[60] Architectural Energy Corporation. Chiller Plant Efficiency. Boulder, CO.; 2008.
[61] Osorio-Tejada J, Tran NN, Hessel V. Techno-environmental assessment of small-scale Haber-Bosch and plasma-assisted ammonia supply chains. Sci Total Environ 2022;826:154162. https://doi.org/10.1016/j.scitotenv.2022.154162.
[62] Peters MS, Timmerhaus KD, West RE. Plant Design and Economics for Chemical Engineers 5th Edition. 5th ed. New York: 2003.
[63] ChemAnalyst. Carbon Black Price Trend and Forecast. Mark Overv Quart End June 2021 2021. https://www.chemanalyst.com/Pricing-data/carbon-black-42 (accessed September 10, 2021).
[64] Towler G, Sinnott R. Economic Evaluation of Projects. In: Butterworth-Heinemann, editor. Chem. Eng. Des. Princ. Pract. Econ. Plant Process Des. Second, Oxford: Elsevier Ltd; 2013, p. 389–429. 10.1016/b978-0-08-096659-5.00009-2.
[65] The Royal Society. Ammonia: zero-carbon fertiliser, fuel and energy store. London: 2020.
[66] ISO. ISO 14040:2006. Environmental management — Life cycle assessment — Principles and framework. vol. 2006. Second edi. Geneva: ISO; 2006.
[67] Azapagic A, Clift R. Allocation of environmental burdens in multiple-function systems. J Clean Prod 1999;7:101–19. 10.1016/S0959-6526(98)00046-8.
[68] ETH. Ecoinvent LCA database. Ecoinvent v38 2022. www.ecoinvent.org (accessed May 22, 2021).
[69] PRé Consultants. SimaPro v9. About SimaPro 2022. www.pre.nl/content/simapro-lca-software (accessed January 16, 2022).
[70] IPCC Working Group 1 I, Stocker TF, Qin D, Plattner G-K, Tignor M, Allen SK, et al. IPCC, 2013: Climate Change 2013: The Physical Science Basis. Contribution of Working Group I to the Fifth Assessment Report of the Intergovernmental Panel on Climate Change. IPCC 2013;AR5.
[71] Hischier R, Weidema B, Althaus H-J, Bauer C, Doka G, Dones R, et al. Implementation of Life Cycle Impact Assessment Methods Data v2.2. 2010.
[72] Bösch ME, Hellweg S, Huijbregts MAJ, Frischknecht R. Applying cumulative exergy demand (CExD) indicators to the ecoinvent database. Int J Life Cycle Assess 2006;12:181. https://doi.org/10.1065/lca2006.11.282.
[73] Götz M, Lefebvre J, Mörs F, McDaniel Koch A, Graf F, Bajohr S, et al. Renewable Power-to-Gas: A technological and economic review. Renew Energy 2016;85:1371–90. https://doi.org/10.1016/J.RENENE.2015.07.066.
[74] Mehta P, Barboun P, Herrera FA, Kim J, Rumbach P, Go DB, et al. Overcoming ammonia synthesis scaling relations with plasma-enabled catalysis. Nat Catal 2018;1:269–75. https://doi.org/10.1038/s41929-018-0045-1.
[75] Gorbanev Y, Engelmann Y, Veer K Van, Vlasov E, Ndayirinde C. Synthesis in a DBD Plasma : Metal Activity and Insights into Mechanisms 2021;11:1230.
[76] Bogaerts A, C. Neyts E. Plasma Technology: An Emerging Technology for Energy Storage. ACS Energy Lett 2018;3:1013–27. 10.1021/acsenergylett.8b00184.
[77] Jardali F, Van Alphen S, Creel J, Ahmadi Eshtehardi H, Axelsson M, Ingels R, et al. NOx production in a rotating gliding arc plasma: potential avenue for sustainable nitrogen fixation. Green Chem 2021;23:1748–57. https://doi.org/10.1039/D0GC03521A.
[78] Van Alphen S, Ahmadi Eshtehardi H, O'Modhrain C, Bogaerts J, Van Poyer H, Creel J, et al. Effusion nozzle for energy-efficient NOx production in a rotating gliding arc plasma reactor. Chem Eng J 2022;443:136529. https://doi.org/10.1016/J.CEJ.2022.136529.
[79] Kelly S, Bogaerts A. Nitrogen fixation in an electrode-free microwave plasma. Joule 2021;5:3006–30. https://doi.org/10.1016/J.JOULE.2021.09.009.
[80] Polak LS, Ovsiannikov AA, Slovetsky DI, Vurzel FB. Theoretical and applied plasma chemistry. Moscow 1975.
[81] Asisov RI, Givotov VK, Rusanov VD, Fridman A. No Title. Sov Phys High Energy Chem (Khimia Vysok Energ 1980;14:336.
[82] Mutel B, Dessaux O, Goudmand P. Energy cost improvement of the nitrogen oxides synthesis in a low pressure plasma. Rev Phys Appliquée 1984;19:461–4. https://doi.org/10.1051/rphysap:01984001906046100.
[83] Takenaka S, Shimizu T, Otsuka K. Complete removal of carbon monoxide in hydrogen-rich gas stream through methanation over supported metal catalysts. Int J Hydrogen Energy 2004;29:1065–73. https://doi.org/10.1016/J.IJHYDENE.2003.10.009.
[84] Han Y-F, Kahlich MJ, Kinne M, Behm RJ. Kinetic study of selective CO oxidation in H2-rich gas on a Ru/γ-Al2O3 catalyst. Phys Chem Chem Phys 2002;4:389–97. https://doi.org/10.1039/B103780N.
[85] Haruta M, Yamada N, Kobayashi T, Iijima S. Gold catalysts prepared by coprecipitation for low-temperature oxidation of hydrogen and of carbon monoxide. J Catal 1989;115:301–9. https://doi.org/10.1016/0021-9517(89)90034-1.
[86] Oh SH, Sinkevitch RM. Carbon monoxide removal from hydrogen-rich fuel cell feedstreams by selective catalytic oxidation. OstiGov 1993;142:1. https://doi.org/10.1006/jcat.1993.1205.
[87] ACCC. Australian Energy Regulator. Gas Mark Prices 2022. https://www.aer.gov.au/wholesale-markets/wholesale-statistics/gas-market-prices (accessed July 9, 2022).
[88] ACCC. Australian Energy Regulator. Annu Vol Weight Aver 30-Minute Prices - Reg 2022. https://www.aer.gov.au/wholesale-markets/wholesale-statistics/annual-volume-weighted-average-30-minute-prices-regions (accessed July 9, 2022).
[89] Chen XY, Vinh-Thang H, Ramirez AA, Rodrigue D, Kaliaguine S. Membrane gas separation technologies for biogas upgrading. RSC Adv 2015;5:24399–448. https://doi.org/10.1039/C5RA00666J.
[90] IEAGHG. Potential for Production With Carbon Dioxide Capture and. Cheltenham: 2013.
[91] Yang M, Baral NR, Anastasopoulou A, Breunig HM, Scown CD. Cost and life-cycle greenhouse gas implications of integrating biogas upgrading and carbon capture technologies in cellulosic biorefineries. Environ Sci Technol 2020;54:12810–9. https://doi.org/10.1021/acs.est.0c02816.
[92] Indrawan N, Thapa S, Wijaya ME, Ridwan M, Park DH. The biogas development in the Indonesian power generation sector. Environ Dev 2018;25:85–99. https://doi.org/10.1016/J.ENVDEV.2017.10.003.
[93] Martín-Hernández E, Guerras LS, Martín M. Optimal technology selection for the biogas upgrading to biomethane. J Clean Prod 2020;267:122032. https://doi.org/10.1016/J.JCLEPRO.2020.122032.
[94] Cozzi L, Gould T, Bouckart S, Crow D, Kim T-Y, McGlade C, et al. World Energy Outlook 2020;2020(2050):1–461.
[95] Long NVD, Kim GS, Tran NN, Lee DY, Fulcheri L, Song Z, et al. Biogas upgrading using ionic liquid [Bmim][PF6] followed by thermal-plasma-assisted renewable hydrogen and solid carbon production. Int J Hydrogen Energy 2021. https://doi.org/10.1016/j.ijhydene.2021.08.231.
[96] Nghiep Tran N, Osorio Tejada J, Razi Asrami M, Srivastava A, Laad A, Mihailescu M, et al. Economic optimization of local australian ammonia production using plasma technologies with green/turquoise hydrogen. ACS Sustain Chem Eng Eng 2021;9:16304–15. https://doi.org/10.1021/acssuschemeng.1c05570.